LANGMUIR

pubs.acs.org/Langmuir

Invited Feature Article

Dynamic Interfacial Regulation by Photodeformable Azobenzene-Containing Liquid Crystal Polymer Micro/Nanostructures

Chongyu Zhu, Yao Lu, Jiahao Sun, and Yanlei Yu*

Cite This: *Langmuir* 2020, 36, 6611−6625

Read Online

ACCESS | Metrics & More | Article Recommendations

ABSTRACT: Photoresponsive materials offer local, temporal, and remote control over their chemical or physical properties under external stimuli, giving new tools for interfacial regulation. Among all, photodeformable azobenzene-containing liquid crystal polymers (azo-LCPs) have received increasing attention because they can be processed into various micro/nanostructures and have the potential to reversibly tune the interfacial properties through chemical and/or morphological variation by light, providing effective dynamic interface regulation. In this feature article, we highlight the milestones in the dynamic regulation of different interfacial properties through micro/nanostructures made of photodeformable azobenzene-containing liquid crystal polymers (azo-LCPs). We describe the preparation of different azo-LCP micro/nanostructures from the aspects of materials and processing techniques and reveal the importance of mesogen orientation toward dynamic interfacial regulation. By introducing our recently developed linear azo-LCP (azo-LLCP) with good mechanical and photoresponsive performances, we discuss the challenge and opportunity with respect to the dynamic light regulation of two- and three-dimensional (2D/3D) micro/nanostructures to tune their related interfacial properties. We have also given our expectation toward exploring photodeformable micro/nanostructures for advanced applications such as in microfluidics, biosensors, and nanotherapeutics.

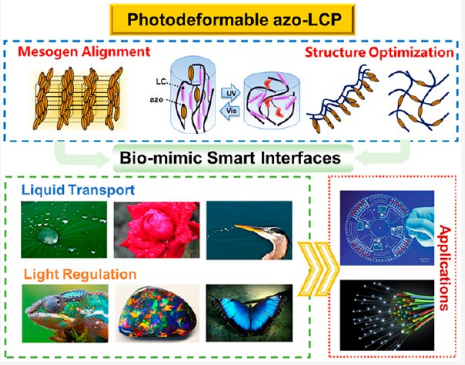

INTRODUCTION

Countless biointerfaces have been created by nature through evolution over millions of years, exhibiting unusual features such as self-cleaning (lotus leaf),[1−3] water collection (beetle elytra),[4,5] and photonic color (Morpho wings).[6,7] Inspired by the chemical components and/or the micro/nanostructured morphologies of these biointerfaces, people have developed various functional materials with useful interfacial properties, demonstrating broad application prospects.[8−11] Typically, irreversible chemical modification or etching of the material surfaces is used to obtain desirable interfacial properties; therefore, it is not facile to adjust their properties after manufacturing.

Different from conventional materials, responsive materials can dynamically adjust their physical and/or chemical properties under external stimuli. With the aid of these materials, interfacial properties such as wettability and reflectivity can now be responsive to pH,[12,13] humidity,[14,15] electricity,[16] magnetic fields,[17−19] heat,[20−22] and light,[23−25] providing various applications including microfluidic devices, controlled drug release, and biosensors.[26] As a clean source, light offers remote and localized control, which is beneficial to the dynamic and accurate regulation over materials.[27−29] Until now, dynamic interfacial regulation by light has been realized through various photoresponsive materials, including photosensitive inorganic oxides,[30−32] small molecular dyes (azobenzene,[33] spiropyran,[34] stilbene,[35] etc.), and their related polymers.[36,37] However, issues such as slow response or limited interfacial property changes during light regulation still hinder their potential applications.

Over the last several decades, photodeformable materials have been explored in various micro/nanostructures for interfacial regulation by light, of which azobenzene-based liquid crystal polymers (azo-LCPs) are a "star".[38] Superior to other photoresponsive materials, azo-LCPs can be shaped into different micro/nanostructures and offer reversible regulation to the chemical environment and/or morphology. Upon light irradiation, the azobenzene molecules in azo-LCPs undergo reversible trans−cis isomerization, generating tunable microscopic chemical properties and interfacial energy change at the micro/nanostructured surface.[38−40] At the same time, the microscopic geometry variation of azobenzene mesogens will be amplified through the polymer entanglements, causing a quick and controllable macroscopic deformation of the micro/

Received: February 29, 2020
Revised: May 24, 2020
Published: May 25, 2020

https://dx.doi.org/10.1021/acs.langmuir.0c00582
Langmuir 2020, 36, 6611−6625

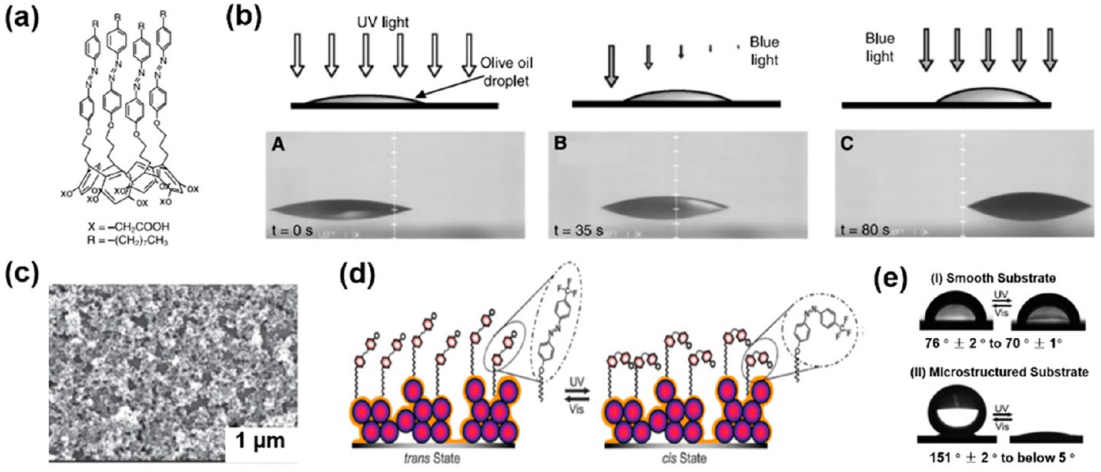

Figure 1. (a) Molecular structure of the azobenzene small-molecule derivative. (b) Light-controlled water transport process at the photoresponsive interface (UV light 365 nm, blue light 436 nm, 1.0 mW cm^{-2}). Adapted with permission from ref 33. Copyright 2000, American Association for the Advancement of Science. (c) SEM image of a microstructured substrate produced by 10 cycles of nanoparticle deposition. (d) Schematic showing the reversible photoisomerization of an azobenzene-coated superhydrophobic surface. (e) Water droplet profiles on (I) smooth and (II) microstructured substrates before and after UV exposure. Adapted with permission from ref 44. Copyright 2010, Royal Society of Chemistry.

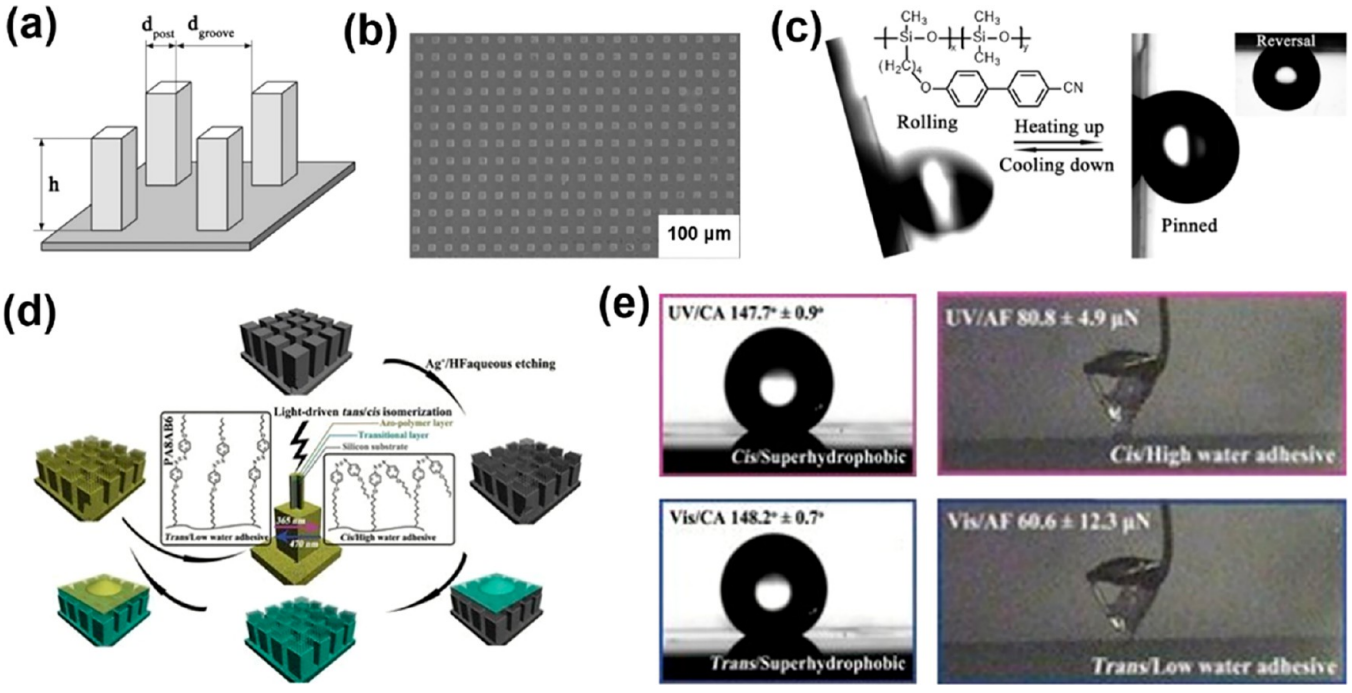

Figure 2. (a) Schematic illustrating the main parameters (d_{post} = 10 μm, d_{groove} = 15 μm, h = 30 μm) of the microposts. (b) Typical SEM image of the polymer-modified surface. (c) Reversible switching of the water droplet mobility from rolling state to pinned state corresponding to the temperature change. Adapted with permission from ref 52. Copyright 2009, John Wiley and Sons. (d) Schematic illustration of the preparation process and the light-driven trans/cis isomerization of the azo-LCP coated micronanoposts. (e) Photoinduced contact angle (CA) and adhesion force changes of this superhydrophobic azo-LCP micronanopost (UV light, 365 nm, 120 mW cm^{-2} for 5 s; visible light, 470 nm, 30 mW cm^{-2} for 10 s). Adapted with permission from ref 53. Copyright 2012, John Wiley and Sons.

nanostructures,[41] which may provide additional interfacial regulation. By manipulating the azo-LCP micro/nanostructures locally using light, we may reversibly fine-tune the related interfacial properties in response to environmental change under a wide regulation range and fast photoresponse, realizing the dynamic interfacial regulation.

In this feature article, we present our recent progress on dynamic interfacial regulation by photoresponsive azo-LCP micro/nanostructures. Focusing on the fabrication strategies and new material development, we investigate the importance of mesogen orientation in azo-LCP micro/nanostructures for liquid and light manipulation. Using our recently developed azo-LCPs with excellent photodeformable performances, we introduce the construction of more complex 2D and 3D azo-LCP micro/nanostructures for dynamic interfacial regulation. We believe the continuous development of azo-LCPs and new fabrication techniques will provide an opportunity for the dynamic control of more complex interface properties by light, solving complicated tasks in real life.

https://dx.doi.org/10.1021/acs.langmuir.0c00582
Langmuir 2020, 36, 6611−6625

DYNAMIC WETTABILITY REGULATION FOR LIQUID MANIPULATION

Interfacial Chemistry Regulation by Azobenzene Molecules. The dynamic regulation of wettability is crucial to realizing droplet manipulation on an open 2D surface, showing potentials in droplet microfluidics,[42] drug screening,[9] cell manipulation,[26] and many other interesting applications.[43] Early in 2000, Ichimura et al. presented the first example of light-driven liquid transport on a photoresponsive flat surface modified by azobenzene small molecules, demonstrating the power of light regulation (Figure 1a,b).[33] Illuminated by alternating ultraviolet (UV) and visible (vis) light, the azobenzene derivatives underwent photoisomerization, generating the variation of interfacial chemistry on the surface. The different ratios of trans and cis azobenzene isomers produced an interfacial energy gradient, driving the motion of liquid droplets (Figure 1b). However, the wettability change at the interface was rather small so that a long manipulation time was needed.

Incorporating micro/nanostructures onto a similar surface system can enhance the variation of wettability. For example, Cho et al. prepared two surfaces coated by the same fluorinated azobenzene small molecules and investigated their wettability changes under UV/vis irradiation (Figure 1c−e).[44] Induced by the photoisomerization of the tethered azobenzene molecules, both surfaces showed a tunable interfacial chemistry change by light, realizing the wettability regulation. Notably, the contact angle (CA) change of the flat surface was 6 ± 1° before and after UV irradiation, while the microstructured film showed a drastic CA change from 151 ± 2° to below 5°, resulting in a photoswitching from superhydrophobicity to superhydrophilicity (Figure 1e). These data suggest that the presence of micro/nanostructures can greatly amplify the photoinduced interfacial change on the surfaces. It can be anticipated that further regulation of the micro/nanostructures may provide an addition pathway to tune the interfacial properties.

Tuning Adhesion by a Responsive Polymer Coating. It has been known that the surfaces of lotus leaves and rose petals are based on similar biomaterials but have opposite adhesion properties. The former is the Wenzel[45] state with superhydrophobic and low adhesion, and the latter is the Cassie[46] state with superhydrophobic and high adhesion. The adhesion difference is mainly induced by the different morphologies on these surfaces.[47−49] Taking inspiration from these biological micro/nanostructures, people have now acquired many responsive micro/nanostructures with unique interfacial properties for liquid manipulation.[50,51] For example, Jiang et al. manufactured a responsive surface by spin-coating a thermoresponsive liquid crystal polymer (LCP) onto a silicon wafer with arrayed microposts (Figure 2a−c).[52] By manipulating the phase transition of the thermoresponsive LCP on the surface via the heating and cooling process, they realized a reversible roughness and interfacial chemistry control of the microposts to tune the interfacial adhesion (Figure 2c), exhibiting the nonloss transport of liquid droplets for droplet microfluidics, self-cleaning surfaces, droplet sorting, and so forth.

In comparison to thermoresponsive LCPs, azobenzene containing polymers (azo-polymers) allow for a precise and athermal manipulation, providing local interfacial changes while preventing the evaporation of liquid droplets. Inspired by Jiang's work as mentioned above, we designed a linear-side-chain azo-polymer synthesized from an azobenzene acrylate monomer with a flexible alkyl spacer.[53] By spin-coating this azo-polymer onto a micronanopost-arrayed silicon wafer, we fabricated a photoresponsive composite surface (Figure 2d). Owing to the hydrophobic azo-polymer and the micronanoposts on the surface, the composite exhibited superhydrophobicity with a CA of about 148°. Through this composite, we for the first time realized the interfacial adhesion manipulation for water droplet release by light.

Once the superhydrophobic azo-polymer micronanopost composite was irradiated with UV light (365 nm, 120 mW cm^{-2}) for 5 s, the azobenzene molecules on the surface underwent trans to cis isomerization, leading to the surface chemistry and roughness change on the micronanoposts. As a result, the composite surface exhibited a 25.0−33.3% increase in the interfacial adhesion force (AF) while the CA variation is subtle (Figure 2e). In this way, we demonstrated the pinning of a water droplet smaller than 2 μL, offering a tool for the size screening of water droplets. Moreover, using visible light (470 nm, 30 mW cm^{-2}), we managed to release the pinned water droplet from the micronanopost composite remotely, providing an alternative design for nonloss liquid droplet transfer. However, the surface roughness change was within a few angstroms during light irradiation limited by the poor photodeformability of this azo-polymer and the hard micronanopost silicon wafer base. Replacing this azo-polymer with azo-LCPs may further increase the morphology variation to improve the liquid transport performance upon light irradiation.

Design of Azo-LCP Micro/Nanostructures for Dynamic Interfacial Regulation. To realize the dual interfacial regulation through azo-LCP micro/nanostructures, a macroscopic deformation of azo-LCPs is essential. There are two main mechanisms of azo-LCP deformation (i.e., photoinduced phase transition and photoreorientation, also known as the "Weigert effect", which has been elaborated on in other reviews[54−57]). Briefly, the photoinduced phase transition of azo-LCPs can be triggered by the photothermal or photochemical effect of azobenzene units. In both cases, the mesogen order will decrease and induce a liquid crystal phase-isotropic phase transition of azo-LCPs, leading to the macroscopic deformation. The Weigert effect of azo-LCPs was first discovered in 1919.[58] Under certain light (for example, blue light) irradiation, azobenzene units will go through continuous trans−cis−trans isomerization until they are aligned along the direction of incident light. The reorientation of azobenzene units can be manipulated by changing the direction of the incident light, disrupting the mesogen order in azo-LCPs to realize deformation.

Typically, azo-LCPs with a cross-linked polymer network (azo-CLCPs) are often used, owing to their excellent mechanical strength and large deformability in response to light. Through the cross-linked polymer network, the synergistic effect of aligned mesogens allows azo-CLCPs to amplify the nanoscopic molecular motions from the photoisomerization of azobenzene units into fast, huge, and various macroscopic deformations, including contraction and expansion,[59−61] topographical deformation,[62−64] bending,[38,65] twisting[66] and rolling.[67] The mesogen orientation in these azo-CLCPs plays an important role in controlling these deformations. Thus, various alignment approaches (for example, magnetic field orientation,[68] mechanical stretching,[69] photoalignment,[70] etc.) have been developed to prepare azo-CLCPs accordingly. For example, our group has used a well-

https://dx.doi.org/10.1021/acs.langmuir.0c00582
Langmuir 2020, 36, 6611−6625

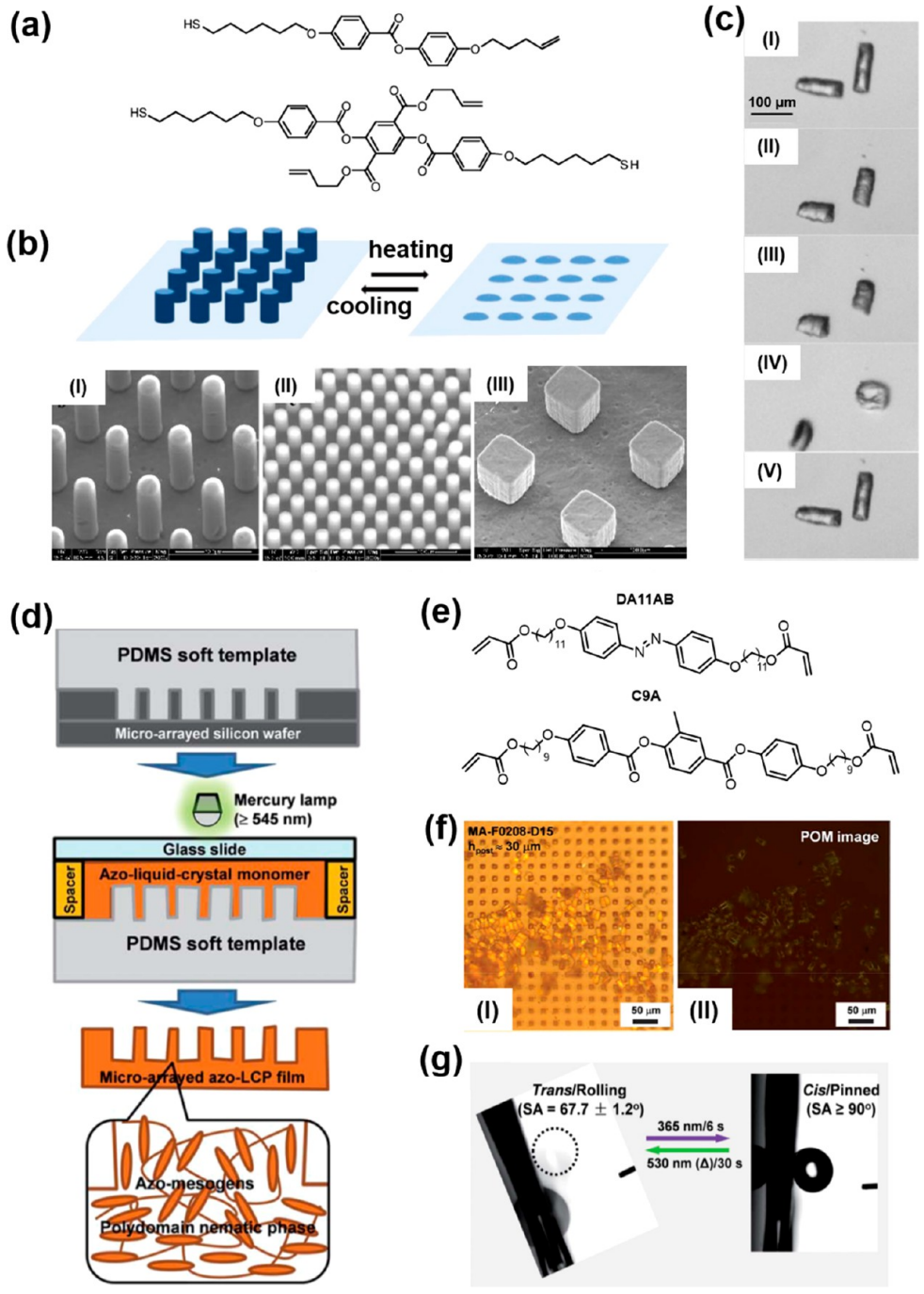

Figure 3. (a) Chemical structures of the monomers used to fabricate the thermoresponsive LCP microarrays by the PDMS soft template. (b) Schematic showing the deformation of the thermoresponsive LCP in response to a temperature variation. (c) SEM images of different microarrays of (I) large cylindrical pillars, (II) small cylindrical pillars, and (III) square pillars by a PDMS soft template. Photographs of a thermoresponsive LCE pillar (I–IV) upon heating to the isotropic state and (V) cooling back to room temperature. Reproduced from ref 76. Copyright 2009, American Chemical Society. (d) Schematic showing the preparation process of the microarrayed azo-CLCP film by the PDMS soft template. (e) Chemical structures of LC monomers (DA11AB and C9A) used to prepare the azo-CLCP film. The molar ratio of DA11AB and C9A in the mixed precursor was 1:4. (f) The cleaved microarrays under (I) the optical microscope and (II) the polarized optical microscope. The width of the microarrays is around 10 μm. The height of the microarrays is around 30 μm. (g) Microscopic profiles of the rolling and pinned water droplets on the microarrayed azo-CLCP surface (UV light: 365 nm, 120 mW cm^{-2} for 6 s; visible light: 530 nm, 30 mW cm^{-2} for 30 s). Adapted with permission from ref 77. Copyright 2012, Royal Society of Chemistry.

arranged carbon nanotube (CNT) layer to guide the azobenzene mesogens, obtaining azo-CLCP/CNT composite films with good mesogen orientation and excellent mechanical properties.[71] Introducing these deformation forms into micro/nanostructures is expected to realize dynamic interfacial regulation by light. However, the mesogen orientation in micro/nanostructures is rather challenging because it is limited by conventional alignment techniques. Thus, it is crucial to make a proper molecular design for azo-CLCPs and select

https://dx.doi.org/10.1021/acs.langmuir.0c00582
Langmuir 2020, 36, 6611−6625

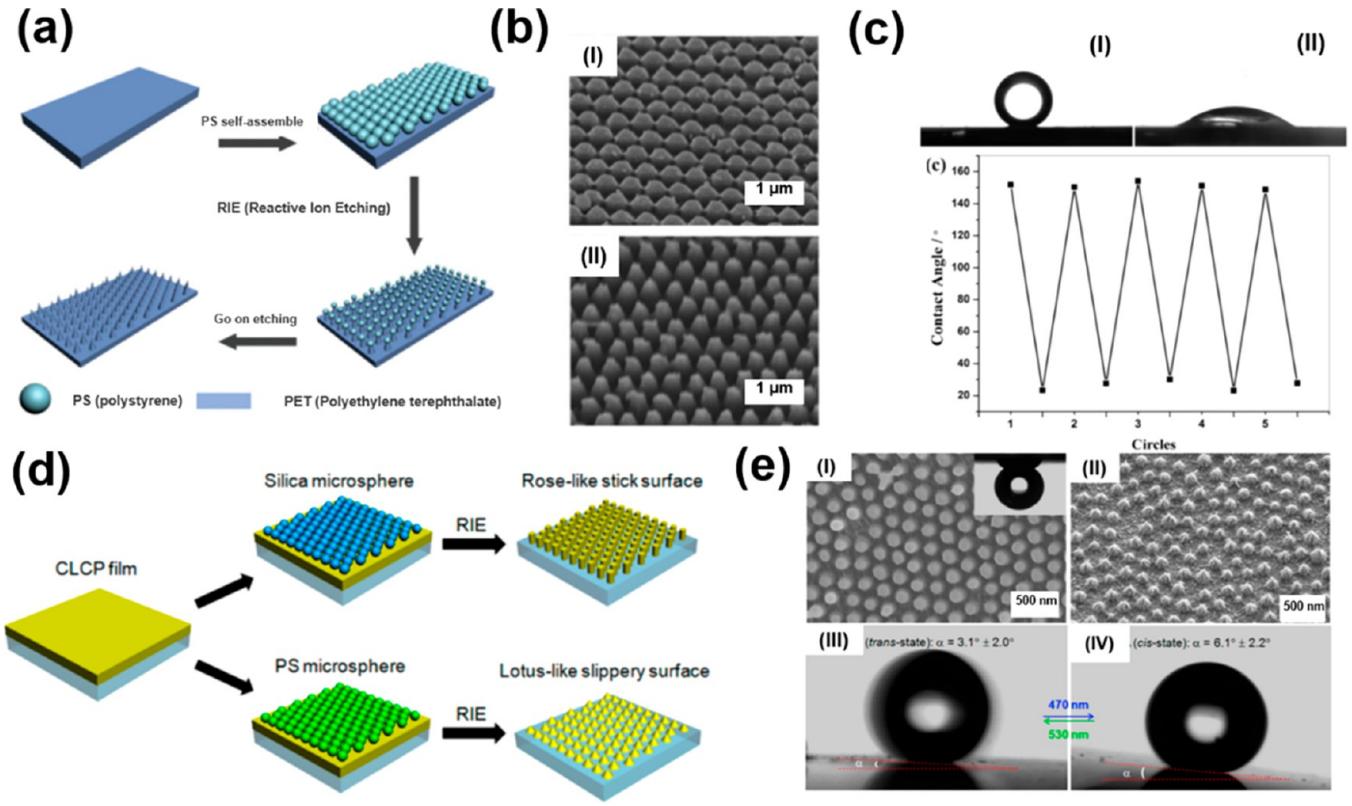

Figure 4. (a) Schematic showing the fabricating process of PET nanocones. (b) Tilted-view SEM images of the (I) joint state and (II) completely isolated state of the PET nanocones presented after etching for 4 and 8 min, respectively. (c) Underwater–oil contact angle (OCA) obtained at (I) 20 and (II) 60 °C. (III) The reversible underwater OCA transition of the PNIPAAm-functionalized PET nanocones at 20 °C (below the LCST of PNIPAAm) and 60 °C (above the LCST of the PNIPAAm). Adapted with permission from ref 83. Copyright 2014 Royal Society of Chemistry. (d) Schematic showing the preparation of microcolumn and microcone arrays by colloidal lithography. (e) (I) Tilted-view SEM image of the submicrocone-arrayed CLCP film. (I inset) Image of a water droplet on the CLCP film turned upside down, indicating high water adhesion. (II) Tilted-view SEM image of the surface of the submicrocone-arrayed CLCP film. (III, IV) SA measurements of a 5 μL water droplet on a submicrocone-arrayed CLCP film in the trans and cis states, respectively (blue light: 470 nm, 120 mW cm^{-2} for 120 s; green light: 530 nm, 30 mW cm^{-2} for 120 s). Reproduced from ref 84. Copyright 2015, American Chemical Society.

suitable processing techniques to prepare micro/nanostructured azo-CLCPs for dynamic interfacial regulation.

Liquid Manipulation by Microarrays. The replication template method is widely applied to prepare complex micro/nanostructures from readily available molds.[72,73] Among all, the PDMS soft template is often used due to its easy reproduction of complex micro/nanostructures including lotus leaves[74] and butterfly wings.[75] In 2009, Keller et al. reported the first preparation of thermoresponsive CLCP microarrays using the PDMS soft template, demonstrating the power of the replication template method in fabricating CLCP microstructures.[76] In their study, the CLCP micropillars on the arrays produced reversible contractions of around 300–400% in response to heat (Figure 3a–c), indicating that the mesogens were well-aligned in the micropillars.

Taking advantage of the replication template method, we designed an azo-CLCP microarray using a PDMS soft template and investigated the dynamic wettability regulation by light (Figure 3d–g).[77] An azo-CLCP precursor was optimized by combining a hydrophobic cross-linkable azobenzene monomer (DA11AB) and a nonazobenzene cross-linker (C9A) (Figure 3e). The precursor possessed a wide temperature range for the nematic phase (40–103 °C on cooling), which ensures that it efficiently fills the microgaps. During this process, the microgaps in the PDMS soft template guided the azobenzene mesogens to align parallel to the surface region of the microarrays (Figure 3f). Compared with a flat film fabricated by the same azo-CLCP, the microarrayed azo-CLCP film surface exhibited superhydrophobicity (CA > 150°) with a smaller slide angle (SA ≈ 37.7°).

Using UV and visible light for illumination, we demonstrated the photoswtiching of a low adhesion state and a high adhesion state of the microarrayed azo-CLCP film. After irradiating the film with UV light (360 nm, 120 mW cm^{-2}) for 6 s, the well-oriented azobenzene mesogens on the surface underwent a cooperative photoisomerization, generating sufficient polarity change and increasing the SA at the interface. Through this microarrayed film, we further realized the noncontact and localized manipulation of the water droplet by light. After 365 nm UV light irradiation, a 2 μL water droplet was pinned on the surface even though the film was in a vertical state (Figure 3g). Subsequently, after the visible light (530 nm, 30 mW cm^{-2}) irradiation for 30 s, the cis-state azobenzene mesogens on the surface returned to the trans-state, reverting the surface into the lower adhesive superhydrophobic state so that the 2 μL water droplet rolled off of the surface when the slant angle of the film reached 67.7°. Due to the fast response and good orientation of these azo-CLCP microarrays, the interfacial regulation time is within a minute, which is beneficial to the real-time control of microfluidics.

Wettability Regulation from Submicro/Nanoarrays. In comparison to the replication template method, colloidal

https://dx.doi.org/10.1021/acs.langmuir.0c00582
Langmuir 2020, 36, 6611–6625

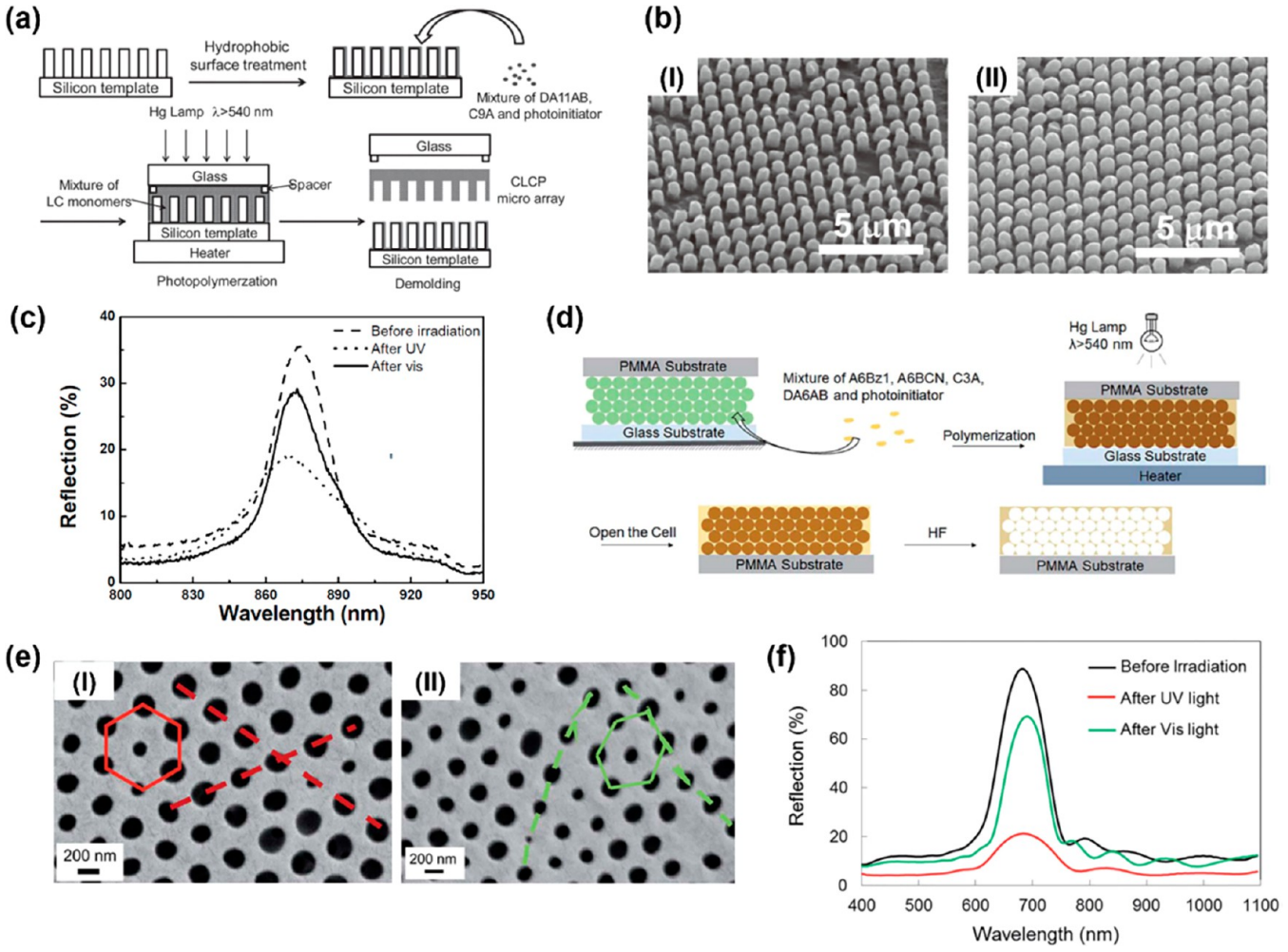

Figure 5. (a) Schematic showing the fabrication of the 2D azo-CLCP microarray. (b) SEM images of the azo-CLCP microcolumns (I) before and (II) after irradiation with UV light. (c) Reflection spectra of the azo-CLCP microarrayed PhC interface under UV light irradiation (365 nm, 20 mW cm^{-2},15 min) and the following visible light irradiation (530 nm, 20 mW cm^{-2}, 5 min) with an angle of incidence of 60°. Adapted with permission from ref 95. Copyright 2012, John Wiley and Sons. (d) Schematic view of fabricating the inverse opal structures using azo-CLCP by the replication technique. (e) SEM images of the inverse opal film (I) before and (II) after UV light irradiation. The red regular hexagon and straight lines represent the arrangement of the holes before UV light irradiation; the green hexagon and lines represent the arrangement of the holes after irradiation with UV light. After UV light irradiation, the shape of the hexagon becomes irregular, and the straight lines have become curves. (f) Reflection spectra of PhC with the inverse opal structure under UV light irradiation (365 nm, 50 mW cm^{-2}, 5 min) and subsequent visible light irradiation (530 nm, 20 mW cm^{-2}, 15 min). Adapted with permission from ref 99. Copyright 2014, Royal Society of Chemistry.

lithography is able to be divided into modules throughout the etching procedure while requiring less manual operations, thus saving time for the mass production of micro/nanostructures.[78−80] By adjusting the photomasks, surfaces with various micro/nanostructures including artificial shark skin,[81] bionic rice,[78] and antireflective moth eyes[82] have been prepared in a highly efficient manner with a silicon wafer through colloidal lithography. Recently, Yang et al. manufactured a nanocone array surface with underwater superoleophobicity and antibioadhesion performance from the colloidal lithography of poly(ethylene terephthalate) (PET), demonstrating the compatibility of colloidal lithography with polymers (Figure 4a−c).[83] However, this technology has not rarely been applied for the construction of phororesponsive azo-LCP micro/nanostructures with tunable interfacial properties.

Therefore, we investigated the fabrication of azo-CLCP micro/nanostructures through the colloidal lithography technique (Figure 4d,e).[84] Instead of the template-guided mesogen orientation during manufacturing for constructing azo-CLCP micro/nanostructures, azo-CLCP films with good mesogen alignment were prepared through conventional mesogen alignment techniques[71] prior to obtaining the micro/nanostructures by colloidal lithography. By using different types of etching masks, we obtained a submicropillar array (diameter of 250 nm) and a submicrocone array (diameter of 400 nm) through colloidal lithography for the first time (Figure 4d). The submicropillar arrays exhibited interfacial properties similar to those of rose petals, while the submicrocone arrays had a lotus-leaf-like surface. Both films have good mesogen orientation and photodeformability. Using these submicroarrays, we managed to regulate the wettability at the interface dynamically by light.

Both films stayed superhydrophobicity before and after illumination. Upon blue light irradiation (470 nm, 120 mW cm^{-2}), the CAs of both interfaces were reduced slightly (~2 to 3°) and recovered after irradiating with green light (530 nm, 30 mW cm^{-2}), mainly owing to the local polarity variation by the photoisomerization of azo-CLCP. In contrast, different adhesion performances were observed from these two

https://dx.doi.org/10.1021/acs.langmuir.0c00582
Langmuir 2020, 36, 6611−6625

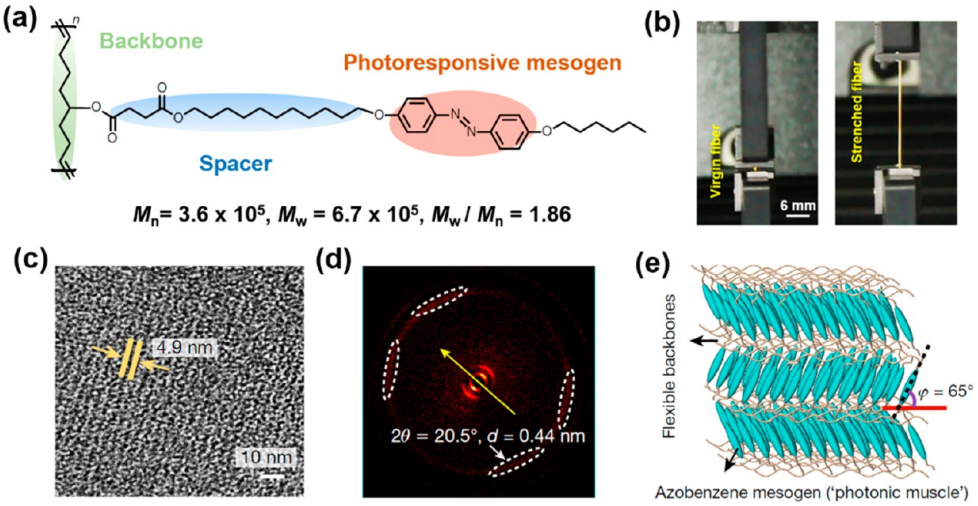

Figure 6. (a) Molecular design strategy of a novel azo-LLCP. (b) Images of the virgin and stretched azo-LLCP fiber. (c) TEM image of the lamellar structure of azo-LLCP. (d) Two-dimensional wide-angle X-ray diffraction pattern of the azo-LLCP film, proving that the azo-LLCP has a lamellar structure and LC phase. (e) Schematic showing the assembled packing structure in the azo-LLCP film. Adapted with permission from ref 100. Copyright 2016, Springer Nature.

submicroarrayed surfaces. The SA of the submicropillar (rose petal) interface remained greater than 90° during the whole process, which is similar to that of the rose petal surface, allowing for the adhesion of a 5 μL water droplet even if the surface was flipped. As for the submicrocone (lotus leaf) CLCP film, the SA value changed from 3.1 ± 2.0° to 6.1 ± 2.2° when irradiated with 470 nm blue light (120 mW cm^{-2}) (Figure 4e). Since the photothermal effect is weak in this process (temperature increased by less than 2 °C after irradiation with 120 mW cm^{-2} blue light for 120 s), the SA variation may be attributed to the photodeformation of azo-CLCP induced by the Weigert effect. It is anticipated that the different morphologies reported in this work may lead to the development of promising applications of photodeformable materials, particularly in microfluidic devices, and self-cleaning windows.

AZO-CLCP PHOTONIC CRYSTALS FOR REFLECTIVITY REGULATION

Photonic crystals (PhC's) have received extensive attention for their unique optical characteristics, where the photonic band gap is the key element. One of the main factors affecting the photonic band gap is the micro/nanostructures of PhC's.[85] By tuning the micro/nanostructures of PhC's, the dynamic interfacial reflectivity regulation can be realized. For example, chameleons can adjust their skin reflection color by changing the nanoscale photonic crystal structures in their epidermal cells.[86] With the development of responsive materials, various PhC's with tunable reflectivity in response to temperature,[87,88] chemical variation,[89] mechanics,[90] light,[91] electricity,[92] and magnetism[93] have been obtained, exhibiting potentials as biological and chemical sensors, photonic inks, color displays, and many optically active components.[94]

Microcolumns by a Silica Template. Fabricating azo-CLCPs into ordered micro/nanostructures such as microarrays, log stack structures, and (inverse) opal structures will produce photoresponsive PhC's with precise and remote regulation of their optical properties.[86] In response to light, the large deformation of the azo-CLCP micro/nanostructures will significantly change the period of Braggs reflection, providing a wide reflectivity regulation range. To demonstrate the regulation of interfacial reflectivty by azo-CLCP, we prepared the first azo-CLCP PhC with microcolumn arrayed structures (Figure 5a–c) through a silicon template.[95] Similar to the procedure of using the PDMS soft template, the azo-CLCP microcolumn-arrayed PhC was obtained by in situ photopolymerization of the precursors containing azobenzene mesogen monomers through a fluorinated silicon template (Figure 5a). The shear force during the casting process helps the azobenzene mesogens to align along the long axis direction of the microcolumns, providing the azo-CLCP with excellent stiffness and response performance. Under UV light (365 nm, 20 mW cm^{-2}), the azobezene mesogens underwent trans–cis isomerization transformation, resulting in the expansion of the microcolumn diameter and the shrinkage in the direction of the long axis, which leads to an interfacial reflection change. As a result, the reflection peak at 870 nm broadened and decreased from 34.3 to 18.9% in response to UV light but recovered when exposed to visible light (530 nm, 20 mW cm^{-2}) (Figure 5c).

Inverse Opal Structures by the Replication Technique. In addition to microcolumn PhC's, inverse opal structures also form excellent PhC's with unique optical properties, such as the existence of a photostop band, adjustable color change, and high reflection intensity. For example, by incorporating different photoresponsive LC derivatives into opal thin films or the SiO_2 inverse opal structures, Sato et al. prepared several photoresponsive PhC interfaces and realized the reversible regulation of their reflection spectra by light.[96−98] However, the base materials used in these PhC's are typically hard so that the deformation from these PhC's is small, making it difficult to achieve large-scale regulation.

Thus, we prepared PhC's with inverse opal structures by azo-CLCP using the replication technique (Figure 5d–f).[99] The precursor containing azobenzene monomers was first injected into the SiO_2 opal film (Figure 5d). After polymerization, the SiO_2 opal template was etched with 1% HF, resulted in an azo-CLCP of inverse opal structures, which realized a switchable reflectivity controlled by alternating UV/vis light irradiation. Confirmed by SEM, the photoinduced deformation of azo-CLCP occurred in response to UV illumination (365 nm, 50

https://dx.doi.org/10.1021/acs.langmuir.0c00582
Langmuir 2020, 36, 6611−6625

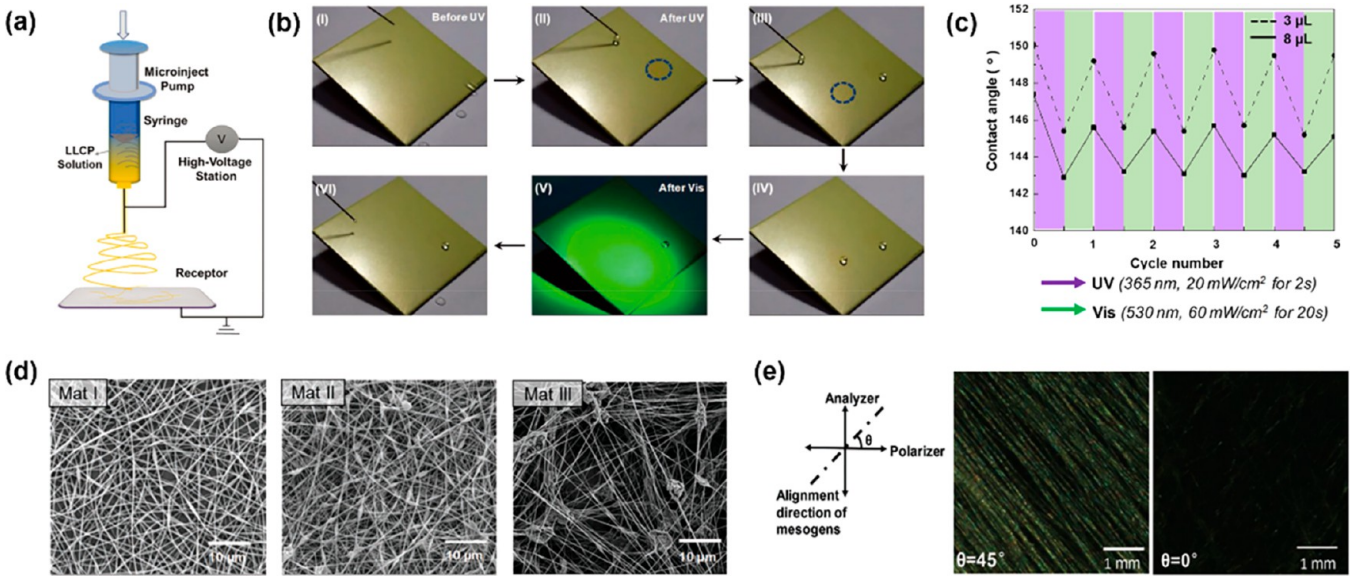

Figure 7. (a) Schematic view of the electrospinning processing. (b) Photographs of directed pinning of moving water droplets of 8 μL on a superhydrophobic mat. (I) Water droplets rolling down the surface of the mat. (II–IV) The circled areas are illuminated with UV light, turning orange owing to the photoisomerization of azobenzene units. Then, the moving droplets could be pinned at the UV-irradiated points. (V, VI) The mat returns to a low AF state after visible-light irradiation, and the droplets slide down smoothly. UV light: 365 nm, 20 mW cm^{-2}; visible light: 530 nm, 60 mW cm^{-2}; size of the mat: 5.0 cm × 5.0 cm. (c) Plot showing the reversible CA change of 3 and 8 μL water on the mat with alternating irradiation with UV and visible light. The surface energy of mat III before UV irradiation is measured to be 45.42 ± 1.42 mN/m and becomes 61.95 ± 0.29 mN/m after UV exposure. (d) Representative FESEM image of nanofiber mats I–III. (e) Polarizing optical microscopy images of nanofibers with parallel alignment. Adapted with permission from ref 110. Copyright 2019, John Wiley and Sons.

mW cm^{-2}), leading to the contraction of the inverse opal structures, which disturbed the regular, periodic porous structure of inverse opal (Figure 5e). As a result, the intensity of the maximum reflection peak at 670 nm decreased to 20% of its original state after 5 min. Although the reflection peak only partially recovered and eventually reached 70% when visible light (530 nm, 20 mW cm^{-2}) was used (Figure 5f), this is the first time that azo-CLCP has been used in the preparation of inverse-opal-structural PhC's. Through the easy operation by light, we realized the dynamic switching of the reflection spectra in azo-CLCP PhC's.

NEW MATERIALS FOR DYNAMIC INTERFACIAL REGULATION: FROM TWO-DIMENSIONAL TO THREE-DIMENSIONAL MICRO/NANOSTRUCTURES

Although micro/nanostructured azo-CLCPs have shown power in the dynamic regulation of different interfacial properties as described above, the limited processability inherited by their cross-linked structures restricts their processing into more complex 2D/3D microstructures. Therefore, an investigation of new azo-LCP materials with excellent processability is needed. Azo-LCPs with linear structures exhibit good processability for micro/nanostructure fabrication. However, the molecular weight of previously reported azo-LCPs with linear structures is low so that they do not have enough chain entanglement to form stable physical network to support themselves with good mechanical properties. Thus, the development of linear azo-LCPs with excellent self-supporting properties and photoresponsiveness will provide new opportunity for the construction of complex micro/nanostructures for simpler interfacial regulation.

In 2016, we developed a novel linear azobenzene-containing liquid crystal polymer (azo-LLCP) with excellent mechanical and photodeformable properties (Figure 6).[100] Synthesized by ring-opening metathesis polymerization (ROMP), a high-molecular-weight azo-LLCP was obtained with a rubber-like polycyclooctene backbone and photoresponsive azobenzene mesogens on the side chains (Figure 6a). The longer spacer connected to each azobenzene unit isolated the hindrance from the main chain,[101−103] allowing for the assembly of azobenzene mesogens into a lamellar structure with the aid of an annealing process (Figure 6c–e). Meanwhile, the lamellar structure of the azo-LLCP along with its high molecular weight provided enough chain entanglement, forming a physical network to strengthen the mechanical properties of the material (Figure 6b). Tensile tests showed that the fiber samples of such azo-LLCP have a moderate elastic modulus (96 ± 19 MPa) and good breaking strength (~20 MPa), which is similar to or even better than that of conventional azo-CLCPs. The microscopic photoisomerization of azobenzene mesogens in this azo-LLCP upon illumination can be amplified through the polymer network, producing a large macroscopic deformation. Thanks to its linear structure, this new azo-LLCP exhibits excellent processability that is comparable to that of other processing techniques such as solution coating and mold processing, allowing for the easy construction of more complex micro/nanostructures for dynamic interfacial regulation.

Electrospun Azo-LLCP Mats for Wettability Regulation. Electrospinning is advantageous in the large-scale continuous and direct preparation of various micro/nanostructures with unique surface roughness and texture.[104] So far, different responsive polymers have been used to construct micro/nanostructured surfaces with tunable wettability.[105−107] Preparing azo-LCP micro/nanostructures via electrospinning will allow for dynamic interfacial regulation over a large area, which is preferred in industrial applications. However, not only azo-LCP but also all LCPs have rarely been fabricated by electrospinning. That is because the conventional cross-linked LCPs are insoluble so that they are incompatible for processing by electrospinning. As for the previously reported linear LCPs, they normally have low molecular weights limited by the polymerization techniques; therefore, they are unable to provide enough mechanical strength nor can they form stable structures during the electrospinning.[108,109]

With our recently developed azo-LLCP, we have successfully prepared photoresponsive superhydrophobic mats on a large scale by electrospinning (Figure 7a).[110] In comparison to the flat azo-LLCP surface with a CA of about 90°, the mats fabricated by the same material through electrospinning have higher hydrophobicity owing to

https://dx.doi.org/10.1021/acs.langmuir.0c00582
Langmuir 2020, 36, 6611−6625

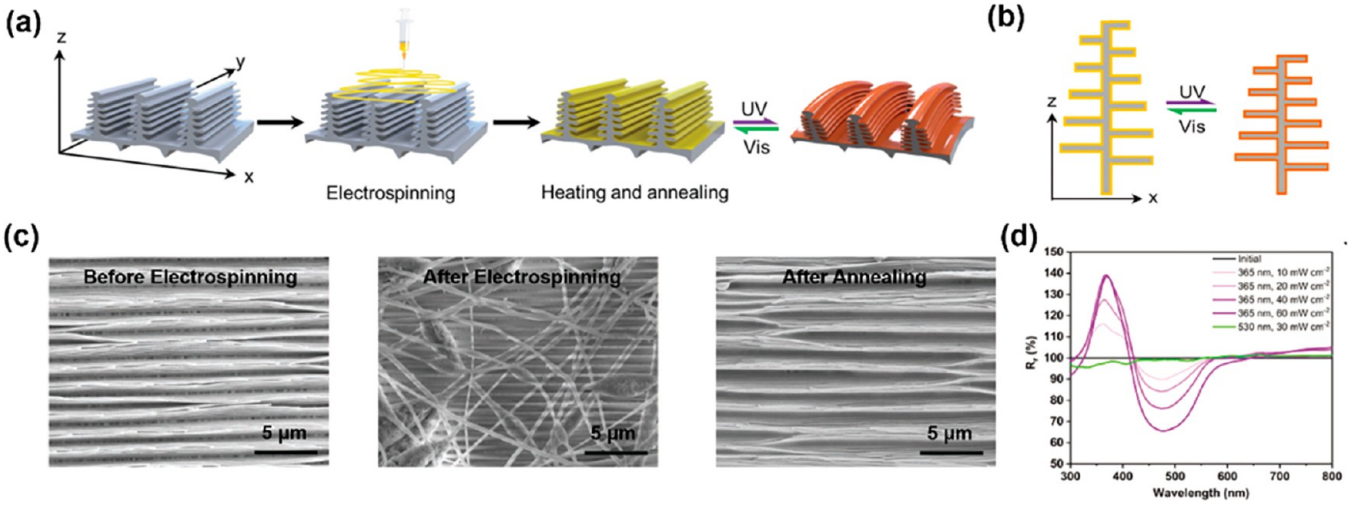

Figure 8. (a) Schematic showing the fabrication of an LLCP-coated *Morpho* butterfly wing (LLCP-MBW) and the reversible photoinduced deformation. For a better understanding of the placement of the MBW in this and the following figures, a coordinate system was set with the *y* axis parallel to the ridges, the *x* axis perpendicular to the ridges, and the *z* axis vertical to the surface. (b) Schematic illustration of the expansion and shrinkage vertical to the ridges induced by UV (365 nm, 10 mW cm^{-2}) and visible light (white light from the microscope) irradiation. (c) SEM photographs showing the top view of microstructures on MBW before electrospinning (left), after electrospinning (middle), and after heating and annealing (right). (d) With the increase in UV intensity, the incident light gradually penetrates the lamellas of the ridges, causing the deformation of microstructures and the increase in the new reflection peak at 397 nm. Adapted with permission from ref 115. Copyright 2018 John Wiley and Sons.

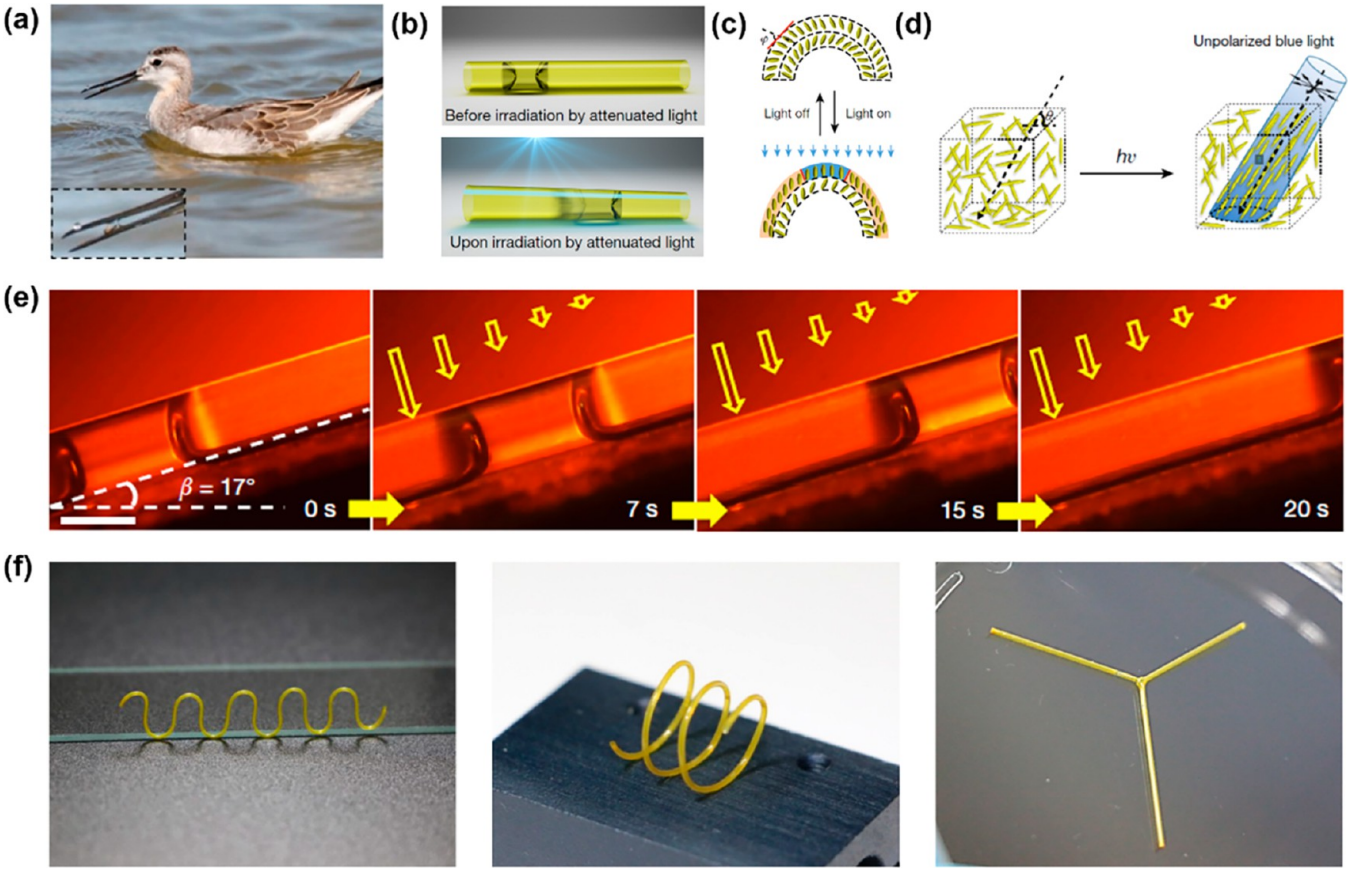

Figure 9. (a) Liquid motion of the bird beak during preying. Adapted with permission from ref 116. Copyright 2008, American Association for the Advancement of Science. (b) Schematics showing the motion of a slug of fully wetting liquid in the photodeformable tubular microactuator (TMA). (c) Schematics showing the reorientation of mesogens in the cross-sectional area of the TMA before and after irradiation with unpolarized blue light. (d) Schematics showing the reorientation of LC mesogens with nonpolarized blue light that is incident at angle θ. Double arrows show the polarization direction of the light. (e) Photographs of the light-driven motion of a silicone oil slug in a TMA tilted up at $\beta = 17°$ (light source: 470 nm blue light, 80 mW cm^{-2}). (f) Photographs of freestanding serpentine, helical, and Y-shaped TMAs. Adapted with permission from ref 100. Copyright 2016, Springer Nature.

https://dx.doi.org/10.1021/acs.langmuir.0c00582
Langmuir 2020, 36, 6611−6625

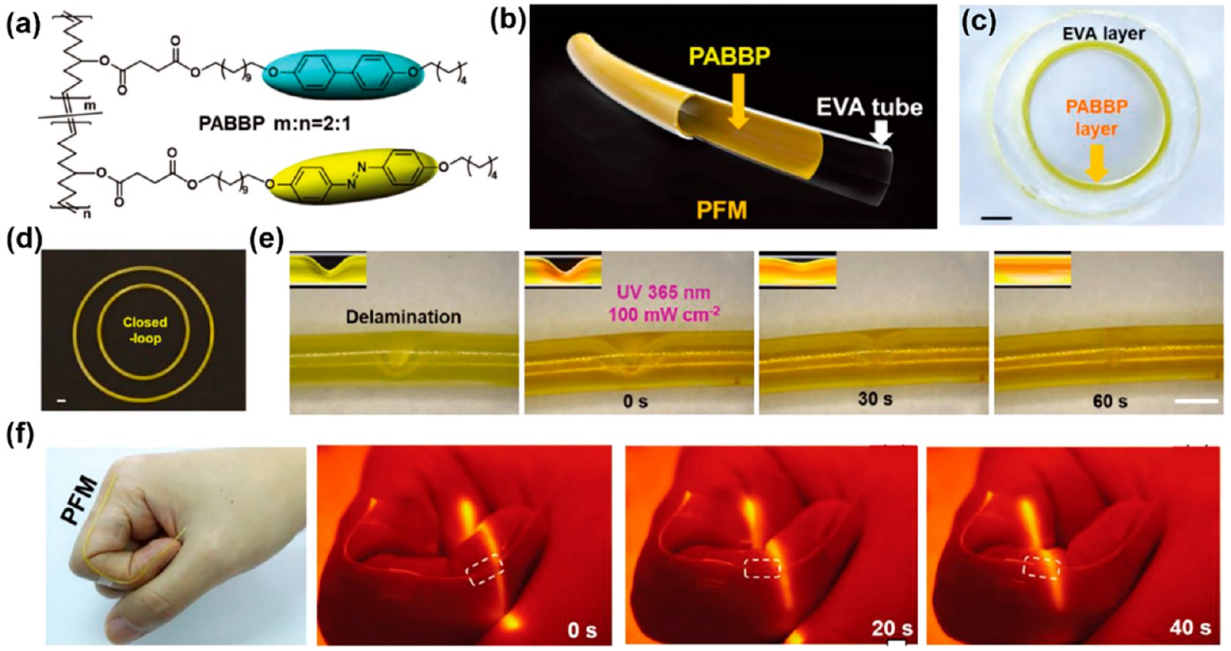

Figure 10. (a) Molecular design of a novel linear azobenzene-containing liquid crystal copolymer (PABBP). (b) Schematic showing the bilayer TMA structure formed by filling an EVA microtube with PABBP. (c) Cross-sectional image of the bilayer TMA. The scale bar is 100 μm. (d) Photograph of a closed-loop microchannel fabricated by the bilayer TMA. (e) Photofluidization-induced healing of the PABBP inner layer. (Inset) Illustration of the healing process. Scale bar: 500 μm. (f) Photograph of the wearable PFM and the photocontrolled liquid transport in the wearable PFM upon irradiation of the 470 nm line light (80 mW cm^{-2}). Adapted with permission from ref 117. Copyright 2019, John Wiley and Sons.

the formation of micro/nanostructures. When the concentration of azo-LLCP solution was reduced from 5 to 1%, the morphology of mats I–III (Figure 7d) was adjustable from fiber to fiber interconnected by particles, giving an increased surface roughness, a larger CA, and a smaller SA. As a result, we obtained two rose petal-like mats (I and II) with high hydrophobicity (CAs of 135 and 139°) and high adhesion and a lotus leaf-like mat (III) that exhibited a superhydrophobic state (CA ≈ 150°) with an SA of 20°.

Upon UV irradiation, a slightly decrease in CA was observed in mat III, resulting from the dipole variation of azobenzene units at the interface during photoisomerization, while the AF and SA were nearly doubled (Figure 7c). Through a detailed analysis, we implied that changes in AF and SA in mat II should be attributed to the dual regulation of micro/nanostructures and the mat surface chemical composition. Induced by the electrospinning process, the mesogens in the azo-LLCP were aligned along the fiber direction, endowing the forming nanofibers with anisotropic photodeformability (Figure 7e). Although no significant morphology change was observed upon UV illumination owing to the randomly distributed azo-LLCP nanofibers on the mat III, the deformation of azo-LLCP nanofibers would change the volume of the presented pores in the micro/nanostructures, leading to the wettability and adhesion changes. In addition, the color of the illuminated spot changed from light yellow to orange, suggesting the trans–cis photoisomerization of azobenzene units occurring on the surface, changing the interfacial chemistry. With these photoresponsive mats, we further demonstrated the pinning of the moving water droplets remotely at the illuminated position, providing a new platform for the active manipulation of discrete droplets on an open surface (Figure 7b).

Reflectivity Regulation from the Azo-LLCP PhC Composite. Compared with the previously mentioned PhC's with microcolumn arrays and inverse opal structures, the replication of more complex natural PhC structures will gain more interesting optical properties. For example, Morpho butterflies wings (MBWs) provide angle-independent blue iridescence, which is hard to obtain from most micro/nanostructured PhC's. Instead of reconstructing the complicated natural structures, installing the natural PhC's with a photoresponse is simpler and will cause most of its optical properties to be inherited while endowing tunability in response to external stimuli.[112,113]

With the aid of photoresponsive materials, people have developed an MBW composite with tunable reflectivity. For example, Zhang et al. developed near-infrared (NIR) photoresponsive PhC's by coating thermoresponsive poly(*N*-isopropylacrylamide) (PNIPAM) coupled with photothermal Fe_3O_4 nanoparticles onto MBW.[114] Triggered by NIR radiation, Fe_3O_4 nanoparticles converted light energy into heat within 10 s, inducing the phase transition of PNIPAM. As a result, the reflection peak red shifted at around 26 nm. Although it is believed that the deformation of the coating on MBW is crucial to tuning the reflectivity from the MBW composite, no deformation of the MBW hierarchical structures has been observed so far due to the weak mechanical properties or low deformation capacity of the coating.[111]

To get a better understanding of the relationship between the micro/nanostructural deformation and reflection changes, we prepared a photodeformable MBW PhC composite with tunable reflectivity by electrospinning the azo-LLCP onto the natural MBW (Figure 8a).[115] Instead of chemical modification methods, a uniform layer of azo-LLCP with good mesogen alignment was attached to the MBW surface through electrospinning, followed by the annealing process (Figure 8c). The delicate hierarchical structures of MBW were preserved with no significant damage thanks to the mild electrospinning process. Due to the excellent mechanical properties and photoinduced deformation of this azo-LLCP, we observed the reversible deformation of the MBW micro/nanostructures including lamella spacing, ridges, and complete scales regulated by UV light (365 nm, 60 mW cm^{-2}, 10 s) for the first time (Figure 8b). The hierarchical deformation of such a responsive MBW composite interface further induced a blue shift in the reflection peak (70 nm) and a remarkable change in reflectance (40%) (Figure 8d). We believe the fabrication of natural PhC's into responsive composites through this approach will provide opportunities for the construction of other phototunable natural PhC's, enriching more important optical features in the application of pigments, cosmetics, and sensors.

Three-Dimensional Tubular Microstructures for Dynamic Interfacial Regulation. Learning from the feeding mechanism in shorebirds, it has been known that a wetting liquid droplet confined in

https://dx.doi.org/10.1021/acs.langmuir.0c00582
Langmuir 2020, 36, 6611–6625

a conical capillary will spontaneously move toward the narrow end. This is due to the asymmetric capillary force caused by the difference in liquid/air interfacial pressure at different curvature pipe diameters.[116] Inspired by this, we proposed a new liquid transport strategy using light-tunable 3D tubular microstructures (Figure 9). By constructing photoresponsive tubular microactuators (TMAs), we may mimic the motion of a bird beak during preying to realize the surface-tension-induced transport by light (Figure 9a–d). However, limited by the processing techniques and the choice of azo-LCPs, the fabrication of tubular microactuators (TMAs) remains challenging.

With the newly developed azo-LLCP, we prepared the first free-standing 3D TMA with good mesogen orientation through the coating of azo-LLCP into a glass capillary template.[100] After being coated with the azo-LLCP, the glass capillary template was etched to obtain the TMA. An additional annealing process was performed to improve the mesogen orientation of the azo-LLCP, thereby forming an ordered lamellar structure coaxially in the TMA wall. Upon irradiation with 470 nm blue light (80 mW cm^{-2}), the azobenzene mesogens underwent continuous trans–cis–trans photoisomerization by the Weigert effect (Figure 9b,c), leading to the reorientation along the direction of incident light. As a result, the thickness of the illuminated part decreased and its diameter was expanded, producing an asymmetrical deformation in the azo-LLCP TMA (Figure 9d). Once the light source was removed, the photodeformation was recovered, exhibiting good reversibility for repeated use.

Through this photodeformable TMA, we successfully applied our new liquid transport strategy and demonstrated the liquid propulsion using light in a 3D microstructure for the first time. Induced by the photoinduced asymmetrical deformation, an asymmetric capillary force was created at both ends of the slug, which propelled the droplet toward the narrow end even in a tilted-up TMA (Figure 9e). Through photoinduced capillary force, a variety of liquids were driven in this TMA, including nonpolar and polar solvents, emulsions, and liquid–solid mixtures, which are widely used in biomedical and chemical applications. Moreover, since the wetting of the inner liquid is the key to generating the photoinduced capillary force, we have added a hydrophilic coating inside the TMA to change the TMA wall from a hydrophobic state to a hydrophilic state. For the first time, we realized the directional transport of water droplets through the dynamic regulation of photoresponsive 3D microstructures by light.

Thanks to the good processability of azo-LLCP, other 3D structures such as S shapes, helix shapes, and Y shapes (Figure 9f) have been easily prepared through the same approach by changing the templates, offering tools for the study of complex microstructures. However, because the etching step is unavoidable in the glass capillary template method, the large-scale preparation of such 3D tubular microstructures remains difficult, which may be an issue for their practical applications in microreactors, all-optical microchips, and micro-optical mechanical systems. In addition, the TMA with a thin layer of azo-LLCP exhibits low mechanical robustness and will be subjected to local instability and postbuckling when applied with an external force.

To explore the alternative fabrication methods and further expand the versatility of our light-controlled liquid transport strategy, we further developed a bilayer TMA by introducing azo-LLCP into a commercially available ethylene-vinyl acetate (EVA) microtube (Figure 10).[117] Because the EVA microtube is not photoresponsive, it requires a larger photodeformation of azo-LLCP to overcome the resistance from EVA. Therefore, we designed and synthesized a modified version of azo-LLCP, a linear azobenzene liquid crystal copolymer (PABBP) incorporating both azobenzene and biphenyl mesogens (Figure 10a). The presence of biphenyl mesogens allows for deeper light penetration through the PABBP material compared with the azo-LLCP of just azobenzene mesogens. More importantly, both mesogens can be coassembled into a smectic C phase, forming lamellar structures after annealing, thus improving the breaking strength (240 ± 25 MPa) of PABBP and guaranteeing it to have better photodeformability.

After filling an EVA microtube with PABBP and then annealing, a photoresponsive flexible bilayer microtube (PFM) of more than 1 m was obtained with good mechanical strength (Figure 10b), which can be knotted or used to hang a 200 g weight without damage. Although the EVA layer in the bilayer PFM is about 4 times as thick as the PABBP layer (Figure 10c), the photoresponsive PABBP layer was able to produce sufficient deformation to drive the outer EVA layer of 100 μm thickness for liquid transport upon irradiation with 470 nm light (120 mW cm^{-2}). As for the slug in the monolayer TMA, various liquids were propelled in the predetermined direction in the PFMs through the photoinduced capillary force induced by the Weigert effect. Through several prototypes such as the parallel array and multiple micropumps, we have demonstrated the potential applications of the PFMs in a straight or composite form.

Moreover, due to the flexibility and mechanical properties of the EVA layer, the photodeformability was preserved in the curved PFMs, allowing for the construction of closed-loop microchannels (Figure 10d), which is advantageous for biological microreactions. The potential of the PFMs to construct wearable devices was further demonstrated through the manipulation of liquid slugs in a PFM attached to the index finger controlled by harmless blue light with low density (Figure 10f). In addition, the photoisomerization of azobenzene units in the linear PABBP upon UV illumination can trigger the photofluidization of the PABBP layer, which is useful for the repair of the delaminated bilayer PFMs, elongating their lifetime (Figure 10e). We anticipate that these 3D bilayer tubular microactuators will find use in smart wearable device, microelectromechanical systems (MEMS), and lab-on-a-chip settings as the photocontrollable components and liquid manipulation tools.

CONCLUSIONS AND OUTLOOK

We have highlighted advances in the dynamic interfacial regulation via 2D and 3D azo-LCP micro/nanostructures by applying light as a stimulus. Taking advantage of the photoresponsive azobenzene mesogens, we have demonstrated that azo-LCP micro/nanostructures can produce reversible chemical and/or morphological variation at the interface, showing advantage in potential applications such as liquid and light manipulation. In particular, the development of new photodeformable azo-LLCPs allows us to fabricate various complex 2D and 3D micro/nanostructures, providing a new tool for the dynamic interfacial regulation by light.

Although most studies described in this feature article focus on the fields of liquid transport and reflectivity manipulation by dynamic interfacial regulation, we foresee that micro/nanostructures generated from photodeformable azo-LCPs will be beneficial to other emerging applications such as antifouling/anti-icing coatings, tissue restoration, and drug delivery. However, the continuous development of new materials as well as new fabricating techniques will still be necessary.

Although photodeformable azo-LCPs that respond to various light wavelengths have been widely developed, most photodeformable azo-LCP micro/nanostructures still require UV light for reversible regulation. The limited penetration depth and the potential damage to the biological samples impede UV light as an ideal stimulus for dynamic interfacial regulation in bioapplications. Therefore, the balance between the biocompatibility and photodeformability will become the future trend in developing new azo-LCPs. The introduction of azo-LCPs that respond to visible light or near-infrared light into micro/nanostructures not only will be attractive for more biorelated applications but also will expand the light stimulation options for dynamic regulation.

Owing to the difficult control of mesogen orientations as well as the limited choice of micro/nanostructures during fabrication, the current morphology variation generated from the azo-LCP micro/nanostructures remains simple, hindering

https://dx.doi.org/10.1021/acs.langmuir.0c00582
Langmuir 2020, 36, 6611–6625

more complex interfacial regulation. With more advanced techniques, easier fabrication can be realized to achieve complex and diverse interfacial regulation of azo-LCP micro/nanostructures. In this way, we expect more research on photodeformable azo-LCP micro/nanostructures tailored to applications mimicking natural structure and function, thus offering remote, efficient, and more precise control during dynamic regulation.

AUTHOR INFORMATION

Corresponding Author

Yanlei Yu − *Department of Materials Science and State Key Laboratory of Molecular Engineering of Polymers, Fudan University, Shanghai 200433, China;* orcid.org/0000-0002-4623-3331

Authors

Chongyu Zhu − *Department of Materials Science and State Key Laboratory of Molecular Engineering of Polymers, Fudan University, Shanghai 200433, China;* orcid.org/0000-0001-6337-178X

Yao Lu − *Department of Materials Science and State Key Laboratory of Molecular Engineering of Polymers, Fudan University, Shanghai 200433, China;* orcid.org/0000-0003-4416-8131

Jiahao Sun − *Department of Materials Science and State Key Laboratory of Molecular Engineering of Polymers, Fudan University, Shanghai 200433, China;* orcid.org/0000-0001-7424-4612

Complete contact information is available at: https://pubs.acs.org/10.1021/acs.langmuir.0c00582

Notes

The authors declare no competing financial interest.

Biographies

Chongyu Zhu is currently working as an assistant professor in the Department of Materials Science at Fudan University, China. He completed his B.Sc. in the Department of Chemistry, Tsinghua University, China and his Ph.D. in the Department of Chemistry, University of Warwick, U.K. Before joining Fudan University, he worked as a postdoctoral researcher in the Department of Materials Science and Engineering at the University of California, Berkeley, United States. He has been working on the development of releasable/responsive polymer materials for biosensors and medical applications.

Yao Lu is currently a Ph.D. student in the Department of Materials Science, Fudan University, China. He received his B.S. degree in the College of Material Science and Technology at Nanjing University of Aeronautics and Astronautics, China in 2014. His research interests focus on the construction of liquid crystal polymer soft actuators for applications in microfluidics.

Jiahao Sun is currently a master's student in the Department of Materials Science, Fudan University, China. He received his B.S. in the College of Environmental and Chemical Engineering at Shanghai University of Electric Power, China in 2014. His research interest focuses on the fabrication of photoresponsive polymers for smart medical devices.

Yanlei Yu is a professor in the Department of Materials Science at Fudan University, China. She graduated in applied chemistry from Anhui University in 1993 and obtained her M.S. in polymer chemistry and physics from the University of Science and Technology of China in 1996. She earned her Ph.D. in environmental chemistry and engineering from Tokyo Institute of Technology and was promoted to full professor at Fudan University in 2004. Her research interests focus

https://dx.doi.org/10.1021/acs.langmuir.0c00582
Langmuir 2020, 36, 6611−6625

on the development of photodeformable smart materials and light-controllable interface materials with photosensitive polymers and liquid crystal polymers.

■ ACKNOWLEDGMENTS

This work was supported financially by the National Natural Science Foundation of China (21734003, 51721002, and 51903054), the Innovation Program of Shanghai Municipal Education Commission (2017-01-07-00-07-E00027), and the Natural Science Foundation of Shanghai (19ZR1404500).

■ REFERENCES

(1) Barthlott, W.; Ehler, N. Raster-Elektronen-mikroskopie der Epidermis-Oberflächen von Spermatophyten. *Trop. Subtrop. Pflanzenwelt.* **1977**, *19*, 367−465.
(2) Neinhuis, C.; Barthlott, W. Characterization and Distribution of Water-Repellent, Self-Cleaning Plant Surfaces. *Ann. Bot.* **1997**, *79*, 667−677.
(3) Barthlott, W.; Neinhuis, C. Purity of the Sacred Lotus, or Escape from Contamination in Biological Surfaces. *Planta* **1997**, *202*, 1−8.
(4) Parker, A. R.; Lawrence, C. R. Water Capture by a Desert Beetle. *Nature* **2001**, *414*, 33−34.
(5) Choo, S.; Choi, H.; Lee, H. Water-Collecting Behavior of Nanostructured Surfaces with Special Wettability. *Appl. Surf. Sci.* **2015**, *324*, 563−568.
(6) Kinoshita, S.; Yoshioka, S.; Miyazaki, J. Physics of Structural Colors. *Rep. Prog. Phys.* **2008**, *71*, 076401.
(7) Vukusic, P.; Sambles, J. R.; Lawrence, C. R.; Wootton, R. J. Quantified Interference and Diffraction in Single Morpho Butterfly Scales. *Proc. R. Soc. London, Ser. B* **1999**, *266*, 1403−1411.
(8) Jin, M.; Feng, X.; Feng, L.; Sun, T.; Zhai, J.; Li, T.; Jiang, L. Superhydrophobic Aligned Polystyrene Nanotube Films with High Adhesive Force. *Adv. Mater.* **2005**, *17*, 1977−1981.
(9) Sun, T.; Qing, G. Biomimetic Smart Interface Materials for Biological Applications. *Adv. Mater.* **2011**, *23*, H57−H77.
(10) Liu, X.; Wei, R.; Hoang, P. T.; Wang, X.; Liu, T.; Keller, P. Reversible and Rapid Laser Actuation of Liquid Crystalline Elastomer Micropillars with Inclusion of Gold Nanoparticles. *Adv. Funct. Mater.* **2015**, *25*, 3022−3032.
(11) Shahsavan, H.; Yu, L.; Jakli, A.; Zhao, B. Smart Biomimetic Micro/nanostructures Based on Liquid Crystal Elastomers and Networks. *Soft Matter* **2017**, *13*, 8006−8022.
(12) Huang, J.; Cheng, F.; Binks, B. P.; Yang, H. pH-Responsive Gas-Water-Solid Interface for Multiphase Catalysis. *J. Am. Chem. Soc.* **2015**, *137*, 15015−15025.
(13) Lee, D.; Seo, J.; Khan, W.; Kornfield, J. A.; Kurji, Z.; Park, S. pH-responsive Aqueous/LC Interfaces Using SGLCP-b-polyacrylic Acid Block Copolymers. *Soft Matter* **2010**, *6*, 1964−1970.
(14) Dai, M.; Picot, O. T.; Verjans, J. M. N.; de Haan, L. T.; Schenning, A. P. H. J.; Peijs, T.; Bastiaansen, C. W. M. Humidity-Responsive Bilayer Actuators Based on a Liquid-Crystalline Polymer Network. *ACS Appl. Mater. Interfaces* **2013**, *5*, 4945−4950.
(15) Wu, T.; Li, J.; Li, J.; Ye, S.; Wei, J.; Guo, J. A Bio-inspired Cellulose Nanocrystal-based Nanocomposite Photonic Film with Hyper-reflection and Humidity-responsive Actuator Properties. *J. Mater. Chem. C* **2016**, *4*, 9687−9696.
(16) Liang, X.; Guo, S.; Chen, M.; Li, C.; Wang, Q.; Zou, C.; Zhang, C.; Zhang, L.; Guo, S.; Yang, H. A Temperature and Electric Field-responsive Flexible Smart Film with Full Broadband Optical Odulation. *Mater. Horiz.* **2017**, *4*, 878−884.
(17) Tian, D.; Zhang, N.; Zheng, X.; Hou, G.; Tian, Y.; Du, Y.; Jiang, L.; Dou, S. X. Fast Responsive and Controllable Liquid Transport on a Magnetic Fluid/Nanoarray Composite Interface. *ACS Nano* **2016**, *10*, 6220−6226.
(18) Guisasola, E.; Baeza, A.; Talelli, M.; Arcos, D.; Moros, M.; de la Fuente, J. M.; Vallet-Regí, M. Magnetic-Responsive Release Controlled by Hot Spot Effect. *Langmuir* **2015**, *31*, 12777−12782.
(19) Brown, P.; Bushmelev, A.; Butts, C. P.; Cheng, J.; Eastoe, J.; Grillo, I.; Heenan, R. K.; Schmidt, A. M. Magnetic Control over Liquid Surface Properties with Responsive Surfactants. *Angew. Chem., Int. Ed.* **2012**, *51*, 2414−2416.
(20) Chen, L.; Liu, M.; Lin, L.; Zhang, T.; Ma, J.; Song, Y.; Jiang, L. Thermal-responsive Hydrogel Surface: Tunable Wettability and Adhesion to Oil at the Water/solid Interface. *Soft Matter* **2010**, *6*, 2708−2712.
(21) Wang, T.; Chen, H.; Liu, K.; Wang, S.; Xue, P.; Yu, Y.; Ge, P.; Zhang, J.; Yang, B. Janus Si Micropillar Arrays with Thermal-Responsive Anisotropic Wettability for Manipulation of Microfluid Motions. *ACS Appl. Mater. Interfaces* **2015**, *7*, 376−382.
(22) Gong, X.; Xiao, Y.; Pan, M.; Kang, Y.; Li, B.; Zhang, S. pH- and Thermal-Responsive Multishape Memory Hydrogel. *ACS Appl. Mater. Interfaces* **2016**, *8*, 27432−27437.
(23) Valli, L.; Giancane, G.; Mazzaglia, A.; Scolaro, L. M.; Conoci, S.; Sortino, S. Photoresponsive Multilayer Films by Assembling Cationic Amphiphilic Cyclodextrins and Anionic Porphyrins at the Air/Water Interface. *J. Mater. Chem.* **2007**, *17*, 1660−1663.
(24) Sumaru, K.; Ohi, K.; Takagi, T.; Kanamori, T.; Shinbo, T. Photoresponsive Properties of Poly(N-isopropylacrylamide) Hydrogel Partly Modified with Spirobenzopyran. *Langmuir* **2006**, *22*, 4353−4356.
(25) Takahashi, Y.; Fukuyasu, K.; Horiuchi, T.; Kondo, Y.; Stroeve, P. Photoinduced Demulsification of Emulsions Using a Photo-responsive Gemini Surfactant. *Langmuir* **2014**, *30*, 41−47.
(26) Liu, H.; Li, Y.; Sun, K.; Fan, J.; Zhang, P.; Meng, J.; Wang, S.; Jiang, L. Dual-Responsive Surfaces Modified with Phenylboronic Acid-Containing Polymer Brush to Reversibly Capture and Release Cancer Cells. *J. Am. Chem. Soc.* **2013**, *135*, 7603−7609.
(27) Ikeda, T.; Nakano, M.; Yu, Y.; Tsutsumi, O.; Kanazawa, A. Anisotropic Bending and Unbending Behavior of Azobenzene Liquid-Crystalline Gels by Light Exposure. *Adv. Mater.* **2003**, *15*, 201−205.
(28) Wei, J.; Yu, Y. Photodeformable Polymer Gels and Crosslinked Liquid-crystalline Polymers. *Soft Matter* **2012**, *8*, 8050−8059.
(29) Qing, X.; Qin, L.; Gu, W.; Yu, Y. Deformation of Cross-linked Liquid Crystal Polymers by Light-from Ultraviolet to Visible and Infrared. *Liq. Cryst.* **2016**, *43*, 2114−2135.
(30) Tadanaga, K.; Morinaga, J.; Matsuda, A.; Minami, T. Superhydrophobic-Superhydrophilic Micropatterning on Flowerlike Alumina Coating Film by the Sol-Gel Method. *Chem. Mater.* **2000**, *12*, 590−592.
(31) Lai, Y.; Lin, C.; Huang, J.; Zhuang, H.; Sun, L.; Nguyen, T. Markedly Controllable Adhesion of Superhydrophobic Spongelike Nanostructure TiO_2 Films. *Langmuir* **2008**, *24*, 3867−3873.
(32) Wang, S.; Feng, X.; Yao, J.; Jiang, L. Controlling Wettability and Photochromism in a Dual-Responsive Tungsten Oxide Film. *Angew. Chem., Int. Ed.* **2006**, *45*, 1264−1267.
(33) Ichimura, K. Light-Driven Motion of Liquids on a Photo-responsive Surface. *Science* **2000**, *288*, 1624−1626.
(34) Nayak, A.; Liu, H.; Belfort, G. An Optically Reversible Switching Membrane Surface. *Angew. Chem., Int. Ed.* **2006**, *45*, 4094−4098.
(35) Driscoll, P. F.; Purohit, N.; Wanichacheva, N.; Lambert, C. R.; McGimpsey, W. G. Reversible Photoswitchable Wettability in Noncovalently Assembled Multilayered Films. *Langmuir* **2007**, *23*, 13181−13187.
(36) Nicoletta, F. P.; Cupelli, D.; Formoso, P.; De Filpo, G.; Colella, V.; Gugliuzza, A. Light Responsive Polymer Membranes: A Review. *Membranes* **2012**, *2*, 134−197.
(37) Kollarigowda, R. H. Review on Photo-Responsive Polymeric Interfaces in Biomedical Applications. *J. Biomimetics, Biomater. Biomedical Eng.* **2016**, *27*, 44−54.
(38) Yu, Y.; Nakano, M.; Ikeda, T. Directed Bending of a Polymer Film by Light. *Nature* **2003**, *425*, 145.
(39) Ikeda, T.; Mamiya, J.; Yu, Y. Photomechanics of Liquid-Crystalline Elastomers and Other Polymers. *Angew. Chem., Int. Ed.* **2007**, *46*, 506−528.
(40) Jiang, Z.; Xu, M.; Li, F.; Yu, Y. Red-Light-Controllable Liquid-Crystal Soft Actuators via Low-Power Excited Upconversion Based on

https://dx.doi.org/10.1021/acs.langmuir.0c00582
Langmuir 2020, 36, 6611−6625

TripleT-Triplet Annihilation. *J. Am. Chem. Soc.* **2013**, *135*, 16446−16453.
(41) Yu, H.; Ikeda, T. Photocontrollable Liquid-Crystalline Actuators. *Adv. Mater.* **2011**, *23*, 2149−2180.
(42) Stratakis, E.; Ranella, A.; Fotakis, C. Biomimetic Micro/nanostructured Functional Surfaces for Microfluidic and Tissue Engineering Applications. *Biomicrofluidics* **2011**, *5*, 013411.
(43) Zhang, Y.; Xia, H.; Kim, E.; Sun, H. Recent Developments in Superhydrophobic Surfaces with Unique Structural and Functional Properties. *Soft Matter* **2012**, *8*, 11217−11231.
(44) Lim, H. S.; Lee, W. H.; Lee, S. G.; Lee, D.; Jeon, S.; Cho, K. Effect of Nanostructure on the Surface Dipole Moment of Photoreversibly Tunable Superhydrophobic Surfaces. *Chem. Commun.* **2010**, *46*, 4336−4338.
(45) Wenzel, R. N. Resistance of Solid Surfaces to Wetting by Water. *Ind. Eng. Chem.* **1936**, *28*, 988−994.
(46) Cassie, A. B. D. Contact Angles. *Discuss. Faraday Soc.* **1948**, *3*, 11−16.
(47) Yoshimitsu, Z.; Nakajima, A.; Watanabe, T.; Hashimoto, K. Effects of Surface Structure on the Hydrophobicity and Sliding Behavior of Water Droplets. *Langmuir* **2002**, *18*, 5818−5822.
(48) Nie, H. Y.; Walzak, M. J.; Berno, B.; McIntyre, N. S. Atomic Force Microscopy Study of Polypropylene Surfaces Treated by UV and Ozone Exposure: Modification of Morphology and Adhesion Force. *Appl. Surf. Sci.* **1999**, *144*, 627−632.
(49) Li, Z.; Kong, Q.; Ma, X.; Zang, D.; Guan, X.; Ren, X. Dynamic Effects and Adhesion of Water Droplet Impact on Hydrophobic Surfaces: Bouncing or Sticking. *Nanoscale* **2017**, *9*, 8249−8255.
(50) Gong, X.; Gao, X.; Jiang, L. Recent Progress in Bionic Condensate Microdrop Self-Propelling Surfaces. *Adv. Mater.* **2017**, *29*, 1703002.
(51) Zhang, S.; Huang, J.; Chen, Z.; Lai, Y. Bioinspired Special Wettability Surfaces: From Fundamental Research to Water Harvesting Applications. *Small* **2017**, *13*, 1602992.
(52) Li, C.; Guo, R.; Jiang, X.; Hu, S.; Li, L.; Cao, X.; Yang, H.; Song, Y.; Ma, Y.; Jiang, L. Reversible Switching of Water-Droplet Mobility on a Superhydrophobic Surface Based on a Phase Transition of a Side-Chain Liquid-Crystal Polymer. *Adv. Mater.* **2009**, *21*, 4254−4258.
(53) Li, C.; Zhang, Y.; Ju, J.; Cheng, F.; Liu, M.; Jiang, L.; Yu, Y. In Situ Fully Light-Driven Switching of Superhydrophobic Adhesion. *Adv. Funct. Mater.* **2012**, *22*, 760−763.
(54) Pang, X.; Lv, J.; Zhu, C.; Qin, L.; Yu, Y. Photodeformable Azobenzene-Containing Liquid Crystal Polymers and Soft Actuators. *Adv. Mater.* **2019**, *31*, 1904224.
(55) Ube, T.; Ikeda, T. Photomobile Polymer Materials with Crosslinked Liquid-Crystalline Structures: Molecular Design, Fabrication, and Functions. *Angew. Chem., Int. Ed.* **2014**, *53*, 10290−10299.
(56) Liu, D. Q.; Broer, D. J. Liquid Crystal Polymer Networks: Preparation, Properties, and Applications of Films with Patterned Molecular Alignment. *Langmuir* **2014**, *30*, 13499−13509.
(57) Kularatne, R. S.; Kim, H.; Boothby, J. M.; Ware, T. H. Liquid Crystal Elastomer Actuators: Synthesis, Alignment, and Applications. *J. Polym. Sci., Part B: Polym. Phys.* **2017**, *55*, 395−411.
(58) Weigert, F. Dichroism Induced in a Fine-Grain Silver-Chloride Emulsion by a Beam of Linearly Polarized Light. *Verh. Dtsch. Physic. Ges.* **1919**, *21*, 479−483.
(59) Koerner, H.; White, T. J.; Tabiryan, N. V.; Bunning, T. J.; Vaia, R. A. Photogenerating Work from Polymers. *Mater. Today* **2008**, *11*, 34−42.
(60) Li, M. H.; Keller, P.; Li, B.; Wang, X.; Brunet, M. Light-Driven Side-On Nematic Elastomer Actuators. *Adv. Mater.* **2003**, *15*, 569−572.
(61) Finkelmann, H.; Nishikawa, E.; Pereira, G. G.; Warner, M. A New Opto-Mechanical Effect in Solids. *Phys. Rev. Lett.* **2001**, *87*, 015501.
(62) Liu, D.; Broer, D. J. Self-Assembled Dynamic 3D Fingerprints in Liquid-Crystal Coatings Towards Controllable Friction and Adhesion. *Angew. Chem., Int. Ed.* **2014**, *53*, 4542−4546.
(63) Gelebart, A. H.; Liu, D.; Mulder, D. J.; Leunissen, K. H. J.; van Gerven, J.; Schenning, A. P. H. J.; Broer, D. J. Photoresponsive Sponge-Like Coating for On-Demand Liquid Release. *Adv. Funct. Mater.* **2018**, *28*, 1705942.
(64) Babakhanova, G.; Turiv, T.; Guo, Y.; Hendrikx, M.; Wei, Q.; Schenning, A. P. H. J.; Broer, D. J.; Lavrentovich, O. D. Liquid Crystal Elastomer Coatings with Programmed Response of Surface Profile. *Nat. Commun.* **2018**, *9*, 456.
(65) van Oosten, C. L.; Bastiaansen, C. W. M.; Broer, D. J. Printed Artificial Cilia from Liquid-Crystal Network Actuators Modularly Driven by Light. *Nat. Mater.* **2009**, *8*, 677−682.
(66) Wang, M.; Lin, B.; Yang, H. A Plant Tendril Mimic Soft Actuator with Phototunable Bending and Chiral Twisting Motion Modes. *Nat. Commun.* **2016**, *7*, 13981.
(67) Iamsaard, S.; Anger, E.; Aßhoff, S. J.; Depauw, A.; Fletcher, S. P.; Katsonis, N. Fluorinated Azobenzenes for Shape-Persistent Liquid Crystal Polymer Networks. *Angew. Chem., Int. Ed.* **2016**, *55*, 9908−9912.
(68) Maret, G.; Blumstein, A. Orientation of Thermotropic Liquid-Crystalline Polyesters in High Magnetic Fields. *Mol. Cryst. Liq. Cryst.* **1982**, *88*, 295−309.
(69) White, T. J.; Broer, D. J. Programmable and Adaptive Mechanics with Liquid Crystal Polymer Networks and Elastomers. *Nat. Mater.* **2015**, *14*, 1087−1098.
(70) Beyer, P.; Terentjev, E. M.; Zentel, R. Monodomain Liquid Crystal Main Chain Elastomers by Photocrosslinking. *Macromol. Rapid Commun.* **2007**, *28*, 1485−1490.
(71) Wang, W.; Sun, X.; Wu, W.; Peng, H.; Yu, Y. Photoinduced Deformation of Crosslinked Liquid-Crystalline Polymer Film Oriented by a Highly Aligned Carbon Nanotube Sheet. *Angew. Chem., Int. Ed.* **2012**, *51*, 4644−4647.
(72) Bhushan, B. Bioinspired Structured Surfaces. *Langmuir* **2012**, *28*, 1698−1714.
(73) Sathiyaraj, K.; Harshiny, M.; Nazeema Banu, B.; Rajendran, K.; Kumaran, S. A Review on Techniques to Fabricate Silicon Oxide Arrays for Biomolecules Patterning. *Superlattices Microstruct.* **2011**, *49*, 581−590.
(74) Liu, P.; Gao, Y.; Wang, F.; Yang, J.; Yu, X.; Zhang, W.; Yang, L. Superhydrophobic and Self-Cleaning Behavior of Portland Cement with Lotus-leaf-like Microstructure. *J. Cleaner Prod.* **2017**, *156*, 775−785.
(75) Han, Z.; Li, B.; Mu, Z.; Yang, M.; Niu, S.; Zhang, J.; Ren, L. Fabrication of the Replica Templated from Butterfly Wing Scales with Complex Light Trapping Structures. *Appl. Surf. Sci.* **2015**, *355*, 290−297.
(76) Yang, H.; Buguin, A.; Taulemesse, J.; Kaneko, K.; Méry, S.; Bergeret, A.; Keller, P. Micron-Sized Main-Chain Liquid Crystalline Elastomer Actuators with Ultralarge Amplitude Contractions. *J. Am. Chem. Soc.* **2009**, *131*, 15000−15004.
(77) Li, C.; Cheng, F.; Lv, J.; Zhao, Y.; Liu, M.; Jiang, L.; Yu, Y. Light-controlled Quick Switch of Adhesion on a Micro-arrayed Liquid Crystal Polymer Superhydrophobic Film. *Soft Matter* **2012**, *8*, 3730−3733.
(78) Zhang, X.; Zhang, J.; Ren, Z.; Li, X.; Zhang, X.; Zhu, D.; Wang, T.; Tian, T.; Yang, B. Morphology and Wettability Control of Silicon Cone Arrays Using Colloidal Lithography. *Langmuir* **2009**, *25*, 7375−7382.
(79) Li, Y.; Zhang, J.; Fang, L.; Wang, T.; Zhu, S.; Li, Y.; Wang, Z.; Zhang, L.; Cui, L.; Yang, B. Fabrication of Silicon/Polymer Composite Nanopost Arrays and Their Sensing Applications. *Small* **2011**, *7*, 2769−2774.
(80) Yang, S.; Jang, S. G.; Choi, D.; Kim, S.; Yu, H. K. Nanomachining by Colloidal Lithography. *Small* **2006**, *2*, 458−475.
(81) Liu, Y.; Gu, H.; Jia, Y.; Liu, J.; Zhang, H.; Wang, R.; Zhang, B.; Zhang, H.; Zhang, Q. Design and Preparation of Biomimetic Polydimethylsiloxane (PDMS) Films with Superhydrophobic, Self-Healing and Drag Reduction Properties via Replication of Shark Skin and SI-ATRP. *Chem. Eng. J.* **2019**, *356*, 318−328.

https://dx.doi.org/10.1021/acs.langmuir.0c00582
Langmuir 2020, 36, 6611−6625

(82) Lee, C.; Bae, S. Y.; Mobasser, S.; Manohara, H. A Novel Silicon Nanotips Antireflection Surface for the Micro Sun Sensor. *Nano Lett.* **2005**, *5*, 2438−2442.
(83) Liu, W.; Liu, X.; Fangteng, J.; Wang, S.; Fang, L.; Shen, H.; Xiang, S.; Sun, H.; Yang, B. Bioinspired Polyethylene Terephthalate Nanocone Arrays with Underwater Superoleophobicity and Antibioadhesion Properties. *Nanoscale* **2014**, *6*, 13845−13853.
(84) Zhan, Y.; Zhao, J.; Liu, W.; Yang, B.; Wei, J.; Yu, Y. Biomimetic Submicroarrayed Cross-Linked Liquid Crystal Polymer Films with Different Wettability via Colloidal Lithography. *ACS Appl. Mater. Interfaces* **2015**, *7*, 25522−25528.
(85) Giapis, K. P.; Anderson, C. M. Larger Two-Dimensional Photonic Band Gaps. *Phys. Rev. Lett.* **1996**, *77*, 2949−2952.
(86) Galisteo-López, J. F.; Ibisate, M.; Sapienza, R.; Froufe-Pérez, L. S.; Blanco, Á.; López, C. Self-Assembled Photonic Structures. *Adv. Mater.* **2011**, *23*, 30−69.
(87) Hu, Z.; Lu, X.; Gao, J. Hydrogel Opals. *Adv. Mater.* **2001**, *13*, 1708−1712.
(88) Fei, X.; Lu, T.; Ma, J.; Zhu, S.; Zhang, D. A Bioinspired Poly(N-isopropylacrylamide)/silver Nanocomposite as a Photonic Crystal with Both Optical and Thermal Responses. *Nanoscale* **2017**, *9*, 12969−12975.
(89) Kang, Y.; Walish, J. J.; Gorishnyy, T.; Thomas, E. L. Broad-wavelength-range Chemically Tunable Block-copolymer Photonic Gels. *Nat. Mater.* **2007**, *6*, 957−960.
(90) Foulger, S. H.; Jiang, P.; Lattam, A. C.; Smith, D. W.; Ballato, J. Mechanochromic Response of Poly(ethylene glycol) Methacrylate Hydrogel Encapsulated Crystalline Colloidal Arrays. *Langmuir* **2001**, *17*, 6023−6026.
(91) Yang, B.; Li, L.; Du, K.; Fan, B.; Long, Y.; Song, K. Photo-responsive Photonic Crystals for Broad Wavelength Shifts. *Chem. Commun.* **2018**, *54*, 3057−3060.
(92) Chen, K.; Fu, Q.; Ye, S.; Ge, J. Multicolor Printing Using Electric-Field-Responsive and Photocurable Photonic Crystals. *Adv. Funct. Mater.* **2017**, *27*, 1702825.
(93) Hu, H.; Zhong, H.; Chen, C.; Chen, Q. Magnetically Responsive Photonic Watermarks on Banknotes. *J. Mater. Chem. C* **2014**, *2*, 3695−3702.
(94) Ge, J.; Yin, Y. Responsive Photonic Crystals. *Angew. Chem., Int. Ed.* **2011**, *50*, 1492−1522.
(95) Yan, Z.; Ji, X.; Wu, W.; Wei, J.; Yu, Y. Light-Switchable Behavior of a Microarray of Azobenzene Liquid Crystal Polymer Induced by Photodeformation. *Macromol. Rapid Commun.* **2012**, *33*, 1362−1367.
(96) Kubo, S.; Gu, Z.; Takahashi, K.; Ohko, Y.; Sato, O.; Fujishima, A. Control of the Optical Band Structure of Liquid Crystal Infiltrated Inverse Opal by a Photoinduced Nematic-Isotropic Phase Transition. *J. Am. Chem. Soc.* **2002**, *124*, 10950−10951.
(97) Kubo, S.; Gu, Z.; Takahashi, K.; Fujishima, A.; Segawa, H.; Sato, O. Control of the Optical Properties of Liquid Crystal-Infiltrated Inverse Opal Structures Using Photo Irradiation and/or an Electric Field. *Chem. Mater.* **2005**, *17*, 2298−2309.
(98) Kubo, S.; Gu, Z.; Takahashi, K.; Fujishima, A.; Segawa, H.; Sato, O. Tunable Photonic Band Gap Crystals Based on a Liquid Crystal-Infiltrated Inverse Opal Structure. *J. Am. Chem. Soc.* **2004**, *126*, 8314−8319.
(99) Zhao, J.; Liu, Y.; Yu, Y. Dual-responsive Inverse Opal Films Based on a Crosslinked Liquid Crystal Polymer Containing Azobenzene. *J. Mater. Chem. C* **2014**, *2*, 10262−10267.
(100) Lv, J.; Liu, Y.; Wei, J.; Chen, E.; Qin, L.; Yu, Y. Photocontrol of Fluid Slugs in Liquid Crystal Polymer Microactuators. *Nature* **2016**, *537*, 179−184.
(101) Wilbert, G.; Traud, S.; Zentel, R. Liquid Crystalline Main Chain Polymers Containing the Ferrocene Unit as a Side Group, 2. Variation of the Spacer Length. *Macromol. Chem. Phys.* **1997**, *198*, 3769−3785.
(102) Kaufhold, W.; Finkelmann, H.; Brand, H. R. Nematic Elastomers, 1. Effect of the Spacer Length on the Mechanical Coupling Between Network Anisotropy and Nematic Order. *Makromol. Chem.* **1991**, *192*, 2555−2579.
(103) Aguilera, C.; Bartulin, J.; Hisgen, B.; Ringsdorf, H. Liquid Crystalline Main Chain Polymers with Highly Flexible Siloxane Spacers. *Makromol. Chem.* **1983**, *184*, 253−262.
(104) Nuraje, N.; Khan, W. S.; Lei, Y.; Ceylan, M.; Asmatulu, R. Superhydrophobic Electrospun Nanofibers. *J. Mater. Chem. A* **2013**, *1*, 1929−1946.
(105) Gu, S.; Wang, Z.; Li, J.; Ren, J. Switchable Wettability of Thermo-Responsive Biocompatible Nanofibrous Films Created by Electrospinning. *Macromol. Mater. Eng.* **2010**, *295*, 32−36.
(106) Wang, N.; Zhao, Y.; Jiang, L. Low-Cost, Thermoresponsive Wettability of Surfaces: Poly(N-isopropylacrylamide)/Polystyrene Composite Films Prepared by Electrospinning. *Macromol. Rapid Commun.* **2008**, *29*, 485−489.
(107) Lee, C. H.; Kang, S. K.; Lim, J. A.; Lim, H. S.; Cho, J. H. Electrospun Smart Fabrics that Display pH-responsive Tunable Wettability. *Soft Matter* **2012**, *8*, 10238−10240.
(108) Sharma, A.; Langerwall, J. Electrospun Composite Liquid Crystal Elastomer Fibers. *Materials* **2018**, *11*, 393.
(109) Krause, S.; Dersch, R.; Wendorff, J. H.; Finkelmann, H. Photocrosslinkable Liquid Crystal Main-Chain Polymers: Thin Films and Electrospinning. *Macromol. Rapid Commun.* **2007**, *28*, 2062−2068.
(110) Liu, Y.; Zhu, C.; Zhao, Y.; Qing, X.; Wang, F.; Deng, D.; Wei, J.; Yu, Y. Directed Pinning of Moving Water Droplets on Photo-responsive Liquid Crystal Mats. *Adv. Mater. Interfaces* **2019**, *6*, 1901158.
(111) Peng, W.; Zhu, S.; Zhang, W.; Yang, Q.; Zhang, D.; Chen, Z. Spectral Selectivity of 3D Magnetophotonic Crystal Film Fabricated from Single Butterfly Wing Scales. *Nanoscale* **2014**, *6*, 6133−6140.
(112) Xu, D.; Yu, H.; Xu, Q.; Xu, G.; Wang, K. Thermoresponsive Photonic Crystal: Synergistic Effect of Poly(N-isopropylacrylamide)-co-acrylic Acid and Morpho Butterfly Wing. *ACS Appl. Mater. Interfaces* **2015**, *7*, 8750−8756.
(113) Yang, Q.; Zhu, S.; Peng, W.; Yin, C.; Wang, W.; Gu, J.; Zhang, W.; Ma, J.; Deng, T.; Feng, C.; Zhang, D. Bioinspired Fabrication of Hierarchically Structured, pH-Tunable Photonic Crystals with Unique Transition. *ACS Nano* **2013**, *7*, 4911−4918.
(114) Lu, T.; Pan, H.; Ma, J.; Li, Y.; Zhu, S.; Zhang, D. Near-Infrared Trigged Stimulus-Responsive Photonic Crystals with Hierarchical Structures. *ACS Appl. Mater. Interfaces* **2017**, *9*, 34279−34285.
(115) Qing, X.; Liu, Y.; Wei, J.; Zheng, R.; Zhu, C.; Yu, Y. Phototunable Morpho Butterfly Microstructures Modified by Liquid Crystal Polymers. *Adv. Opt. Mater.* **2019**, *7*, 1801494.
(116) Prakash, M.; Quéré, D.; Bush, J. W. M. Surface Tension Transport of Prey by Feeding Shorebirds: The Capillary Ratchet. *Science* **2008**, *320*, 931−934.
(117) Xu, B.; Zhu, C.; Qin, L.; Wei, J.; Yu, Y. Light-Directed Liquid Manipulation in Flexible Bilayer Microtubes. *Small* **2019**, *15*, 1901847.

https://dx.doi.org/10.1021/acs.langmuir.0c00582
Langmuir 2020, 36, 6611−6625